Entrainment of droplets across shearless turbulent interfaces with and without gravitational effects.

Garrett Good, Sergiy Gerashchenko*, Zellman Warhaft
Cornell University

KITP Santa Barbara 28 April, 2011

- "Entrainment and mixing of water droplets across a shearless turbulent interface with and without gravitational effects" S. GERASHCHENKO, G. GOOD AND Z. WARHAFT. J. Fluid Mech. (2011), vol. 668.

- "Velocity statistics and intermittent transport of inertial particles entraining across a turbulence interface." G. H. GOOD, S. GERASHCHENKO, AND Z. WARHAFT. Under consideration for publication in J. Fluid Mech. February 2011.

* Now at LANL, Los Alamos

Motivation: Cloud entrainment.

Isolated cumulous:
Entrainment throughout
the cloud
depth

Entrainment from above,
sides and at base.
Effects of gravity vary.

Stratocumulus:
Entrainment mainly
from the top

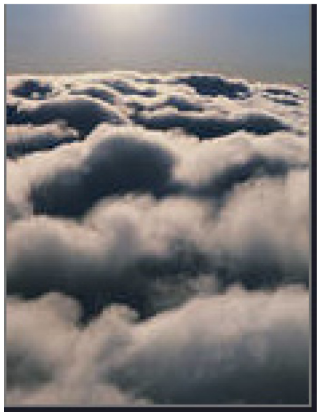

Warm Cumulous

Issues:

Turbulence at the cloud scale: sources, entrainment

Effects of small scale turbulence on droplet growth

Effects of entrainment on droplet growth

Linking fluid dynamics and thermodynamics

Questions:

Are small scale turbulence characteristics in clouds similar to laboratory turbulence?

Does clustering enhance droplet growth? DNS: show clustering---may enhance collision rates, but not guaranteed in real clouds Conflicting results (eg.Pinsky & Khain '04; Riemer & Wexler '05)……

What are the other effects of turbulence? E.g. droplet relative velocity effects on collision efficiency. What are the relative effects of turbulence on collisional growth and condensation growth? (Shaw, Collins, Wang, Malinowski and others)?

What are the relative effects of buoyancy and shear?---shear layer instabilities, convection

How do the different entrainment mechanisms in cumulous (rising plumes) and stratocumulous clouds (plumes impinging on a density interface) affect droplet growth (Grabowski…)?

What affects the width of the droplet spectrum? Instrumental issues. Positive tail of rare, large drops not well measured (Kosinski & Shaw, Brenguier) .Hence effects of small scale turbulence still not clear.

What are the effects of entrainment the droplet distribution and on droplet growth?

What are the effects of gravity on droplet distribution?

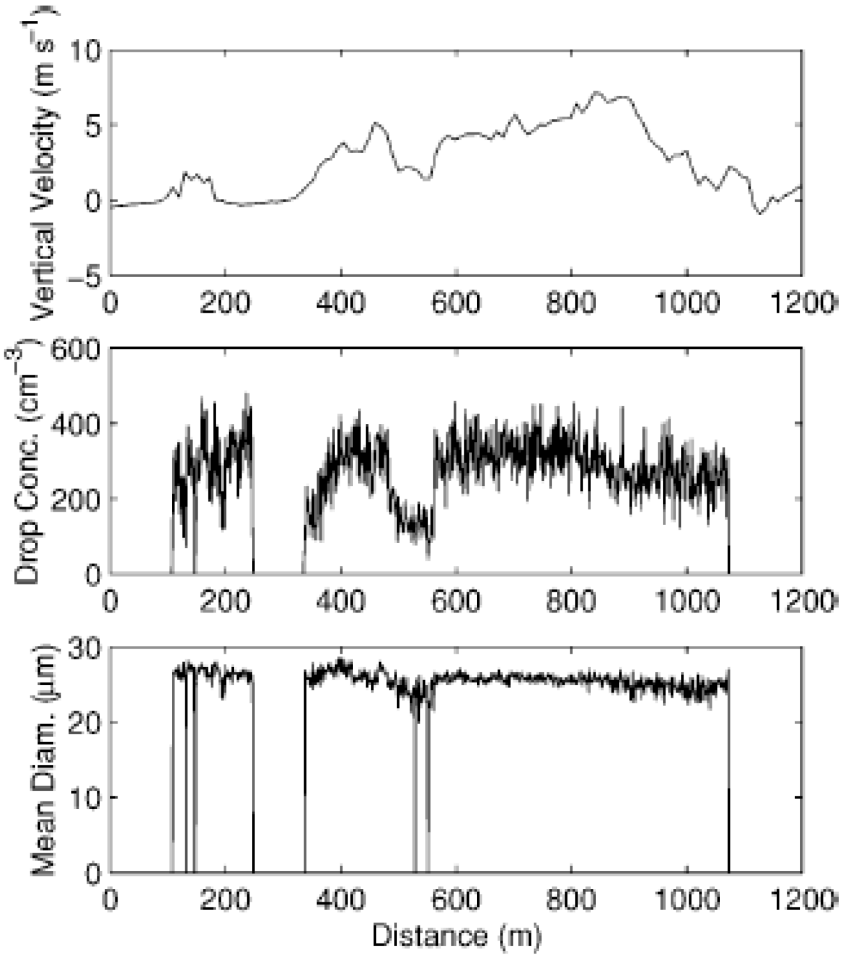

Figure 2 A traverse through a cumulus cloud. The top panel shows the vertical velocity, the middle panel shows droplet number density, and the bottom panel shows mean droplet radius. Note the sharp edges characteristic of the cloud-environment mixing process. Note also that to a large extent the mean radius fluctuates between a constant value and zero, implying that dry and cloudy air are largely segregated during much of the mixing process. Data from the SCMS field experiment, courtesy of J.-L. Brenguier, Meteo-France.

Field experiments: measurements in clouds

Note the very sharp interface with dry air, the relatively constant droplet size, and the existence of shear across the interface in some cases.

from Shaw, Particle-turbulence interactions in atmospheric clouds, ARFM, 35, 183, 2003

Some turbulence characteristics

Taylor scale Reynolds number: $$R_\lambda \equiv \langle u^2 \rangle^{1/2} \lambda / \nu,$$

Taylor microscale defined: $$\langle u^2 \rangle = \lambda^2 \langle (\partial u / \partial x)^2 \rangle$$

Energy dissipation rate : $$\varepsilon \sim \langle u^2 \rangle / \tau \sim \langle u^2 \rangle^{3/2} / \ell,$$

In isotropic turbulence: $$\varepsilon = 15 \nu \langle (\partial u / \partial x)^2 \rangle.$$

Smallest scales of turbulence: $$\eta \equiv (\nu^3/\varepsilon)^{1/4}; \quad \tau_\eta \equiv (\nu/\varepsilon)^{1/2}; \quad v_\eta \equiv (\nu\varepsilon)^{1/4}.$$

Acceleration variance: $$\langle a^2 \rangle = a_0 \varepsilon^{3/2} \nu^{-1/2},$$

If intermittency taken into account: $$\langle a^2 \rangle / \varepsilon^{3/2} \nu^{-1/2} \sim R_\lambda^{0.14}.$$

Cloud measurements

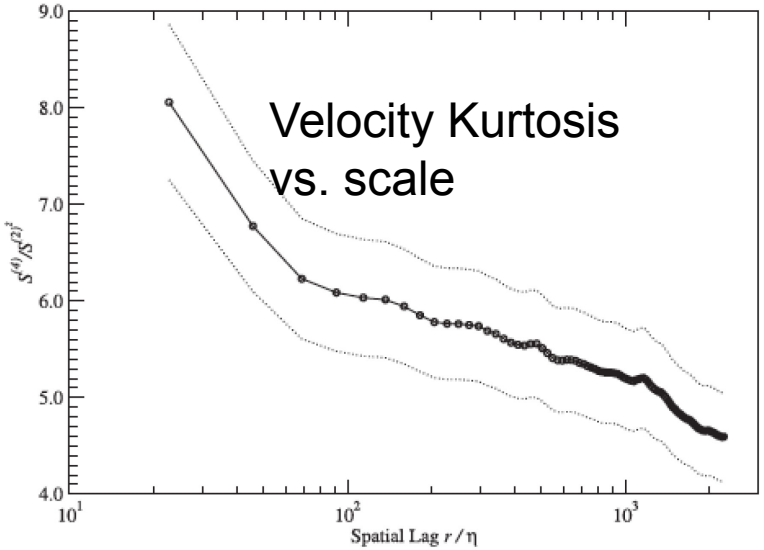

FIG. 10. Kurtosis function $K = S^{(4)}/(S^{(2)})^2$ as a function of the normalized lag r/η. The dotted lines indicate a ±10% range for the statistical sampling uncertainty (see text for more details).

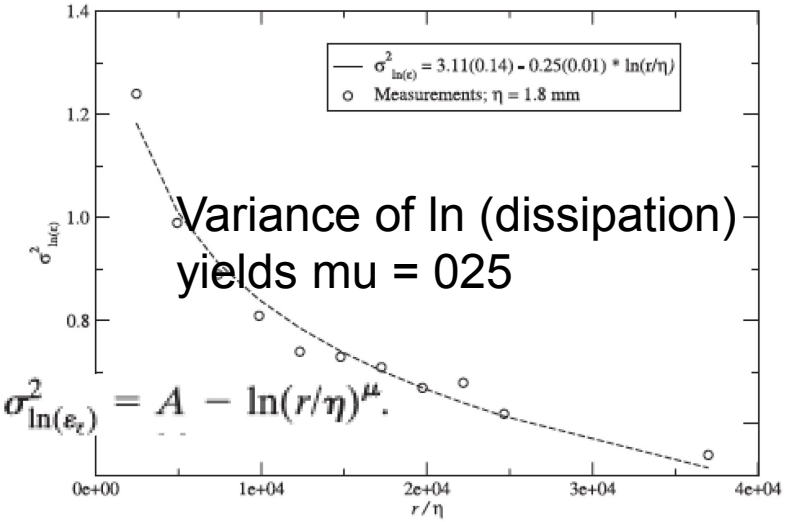

FIG. 11. Variance $\sigma^2_{\ln(\varepsilon_r)}$ as a function of the integration length r normalized with the Kolmogorov length $\eta \approx 1.8$ mm. An integral length scale of $L \approx 100$ m limits $r/\eta < L/\eta \approx 5 \times 10^4$. A logarithmic fit (dashed line) yields an intermittency exponent $\mu = 0.25$ with a standard error of 0.01.

All turbulence measurements in a stratocumulous are consistent with laboratory expts

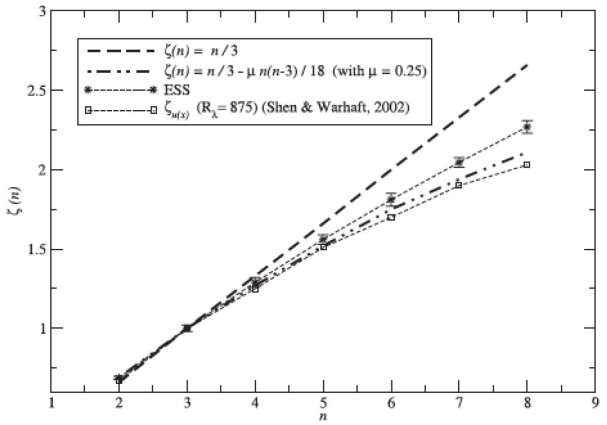

FIG. 9. The scaling exponents $\zeta(n)'$ of the structure functions, as plotted via ESS theory in Fig. 8. Theoretical values for K41 and for K62 with an intermittency factor of $\mu = 0.25$ are shown for reference, together with data derived from wind-tunnel experiments by

Particle parameters.

Note, particles are small (sub-Kolmogorov) , and heavy (density ratio, 840)

Stopping time: $\tau_p \equiv \frac{\rho \langle d^2 \rangle}{18 \mu}$

Stokes Numbers:

$$St_\eta \equiv \tau_p / \tau_\eta \qquad St_\ell \equiv \tau_p / \tau_\ell$$

Settling Parameters

$$Sv_\eta \equiv \tau_p g / u_\eta$$

$$Sv_\ell \equiv \tau_p g / v' \sim \tau_\ell / (\ell / \tau_p g)$$

eddy time scale / Stokes time over dist ℓ

Sv_ℓ large : quiescent terminal velocity

$$Sv \equiv \frac{v_t}{v_\eta} = \frac{\tau_d g}{v_\eta} = \frac{St}{Fr}$$

VS. St

Small Cumulous

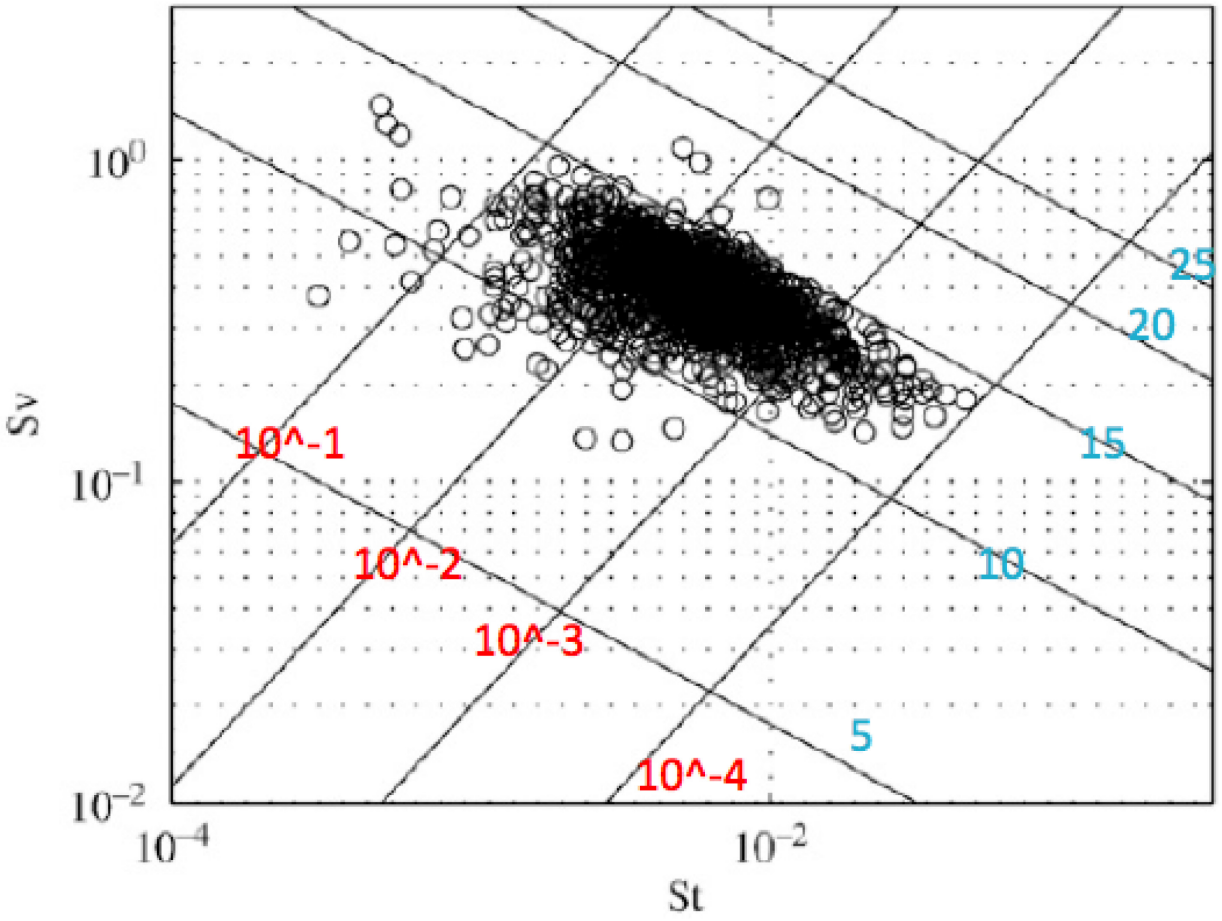

Upward diagonals:
Dissipation rate (m^2/s^3).

Downward diagonals:
Droplet diameters (microns).

NB. THESE ARE AVERAGED VALUES e.g, epsilon

$$Fr \equiv \frac{\sigma_a}{g}$$

$$St \sim d_r^2 \varepsilon^{1/2} \text{ and } Sv \sim d_r^2 \varepsilon^{-1/4}$$

Siebert, Shaw et al.

Clouds

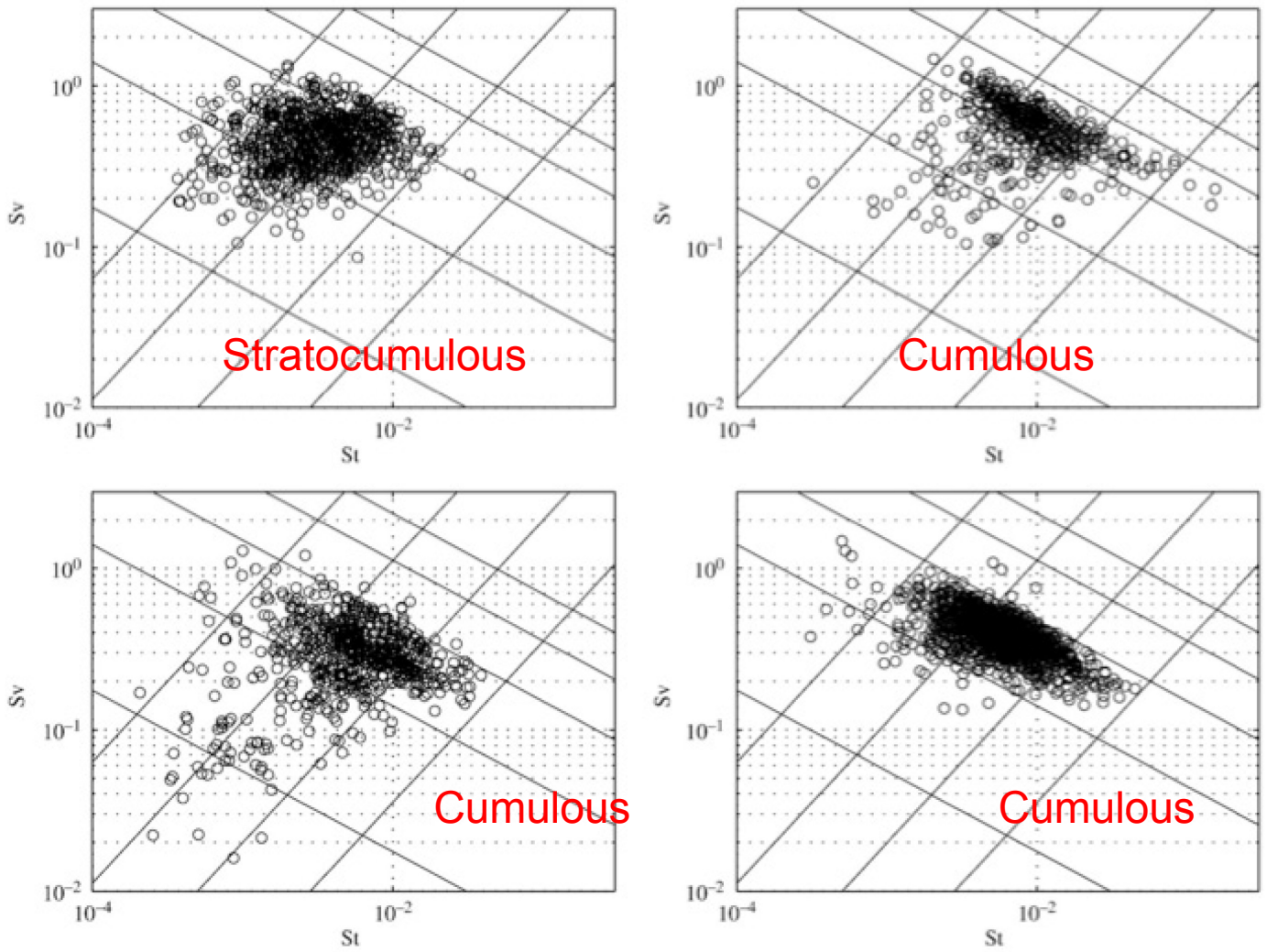

Fig. 9. The distribution of cloud microphysical and turbulence properties in a dimensionless Stokes–settling parameter space. The upper left plot is for a stratocumulus cloud and the remaining three are for small cumulus clouds. Each point represents data in a 1-second (approximately 15 m) average. Diagonal lines with positive slope are contours of constant turbulent energy dissipation rate, ε, at values of 10^{-4}, 10^{-3}, 10^{-2}, and 10^{-1} (lower right to upper left corners). Diagonal lines with negative slope are contours of constant droplet diameter at values of 5, 10, 15, 20 and 25 μm (lower left to upper right corners).

Wind tunnel Experiments:
(a) homogeneous region
(b) entrainment region

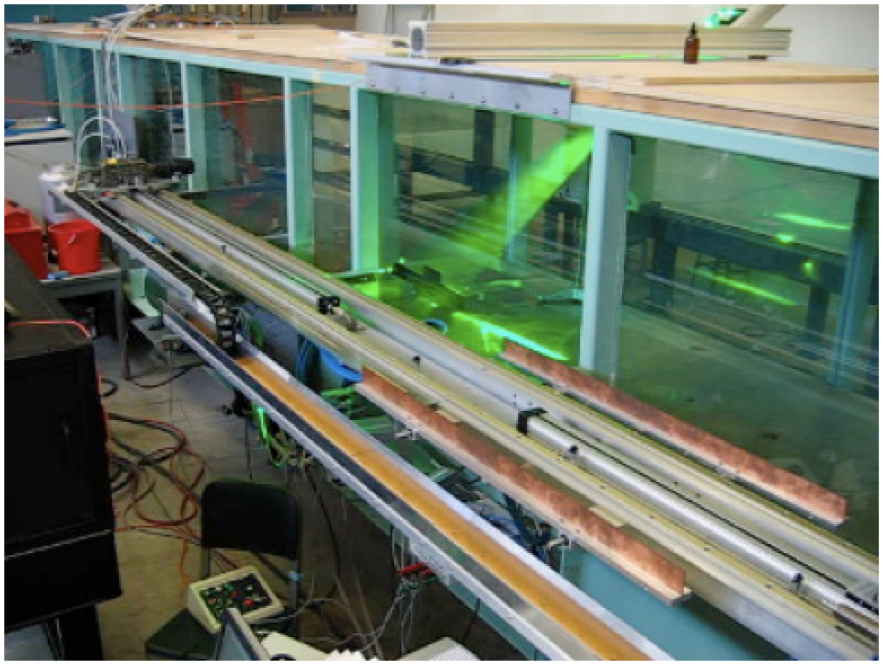

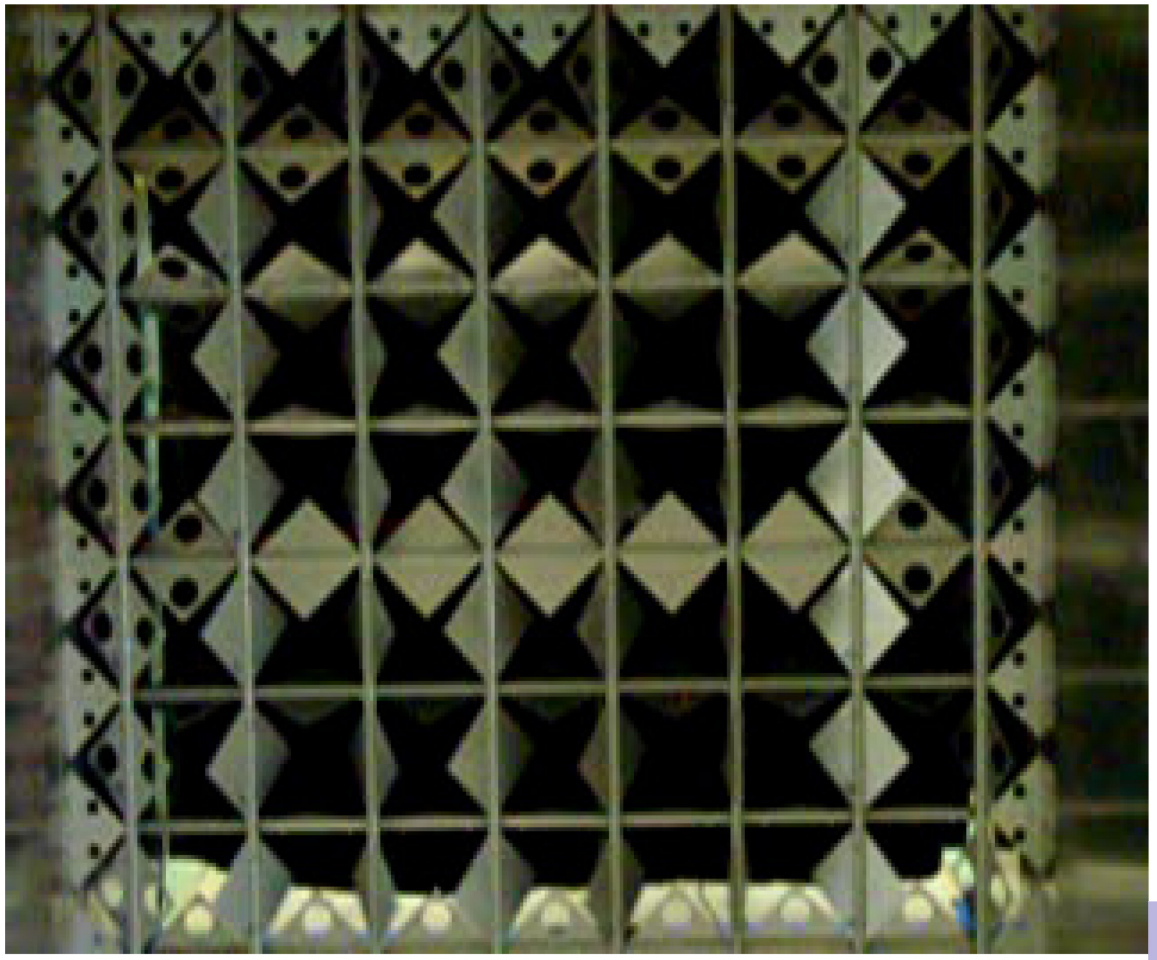

Cornell

Active Grid

M = 163 mm
130 independent position controlled winglets rotate through 180 degrees at up to 2 Hz

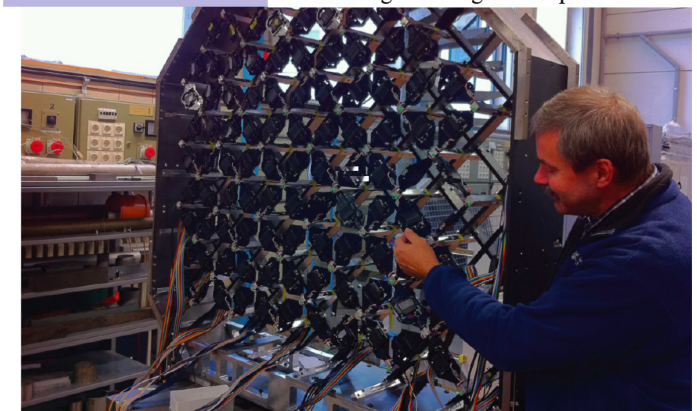

Goettingen

TNI
Turbulent-
Non turbulent
Interface

TTI
Turbulent-
Turbulent
Interface

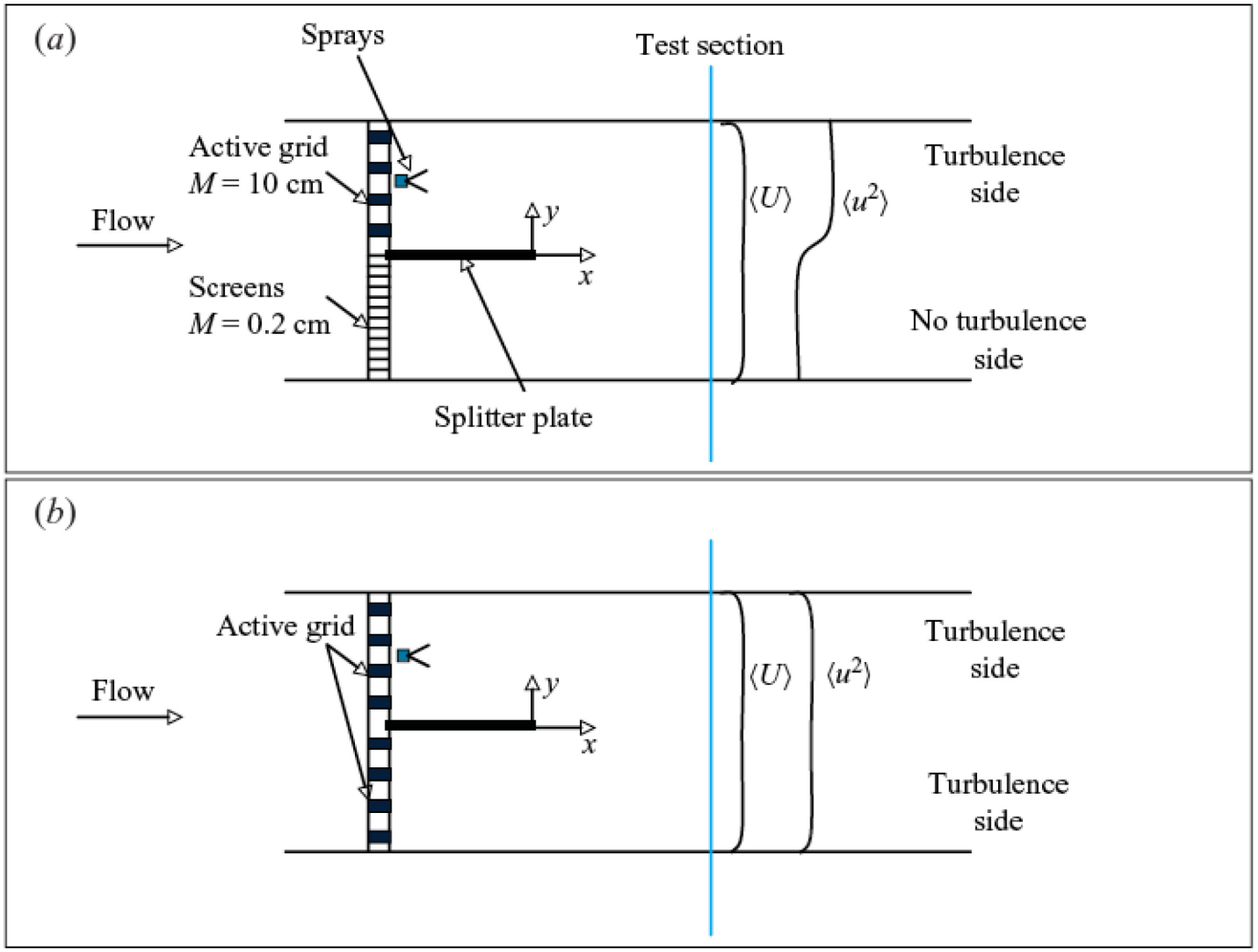

Cornell Wind Tunnel. Grid system may be rotated 90 and 180 degrees: Gravity can aid, inhibit or not affect entrainment.

No Shear.

Smoke visualization

TNI : Turbulent-non turbulent interface

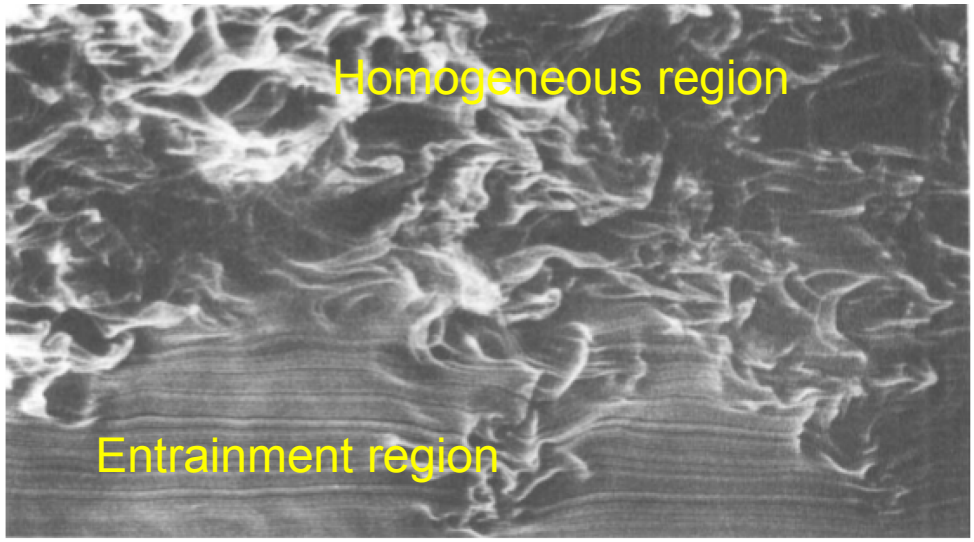

g

g-

g+ homogeneous turbulence at the top.

Particles always injected into turbulent region

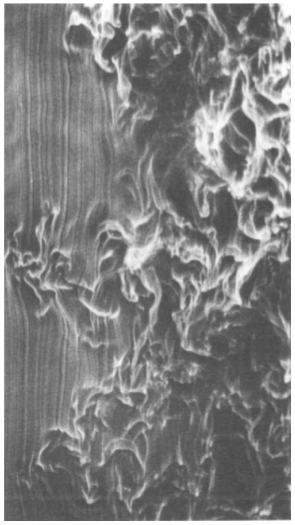

g0

No convection, no phase changes, no collisions

Jayesh & Warhaft, JFM, 277, 23, 1994

(a)

(b)

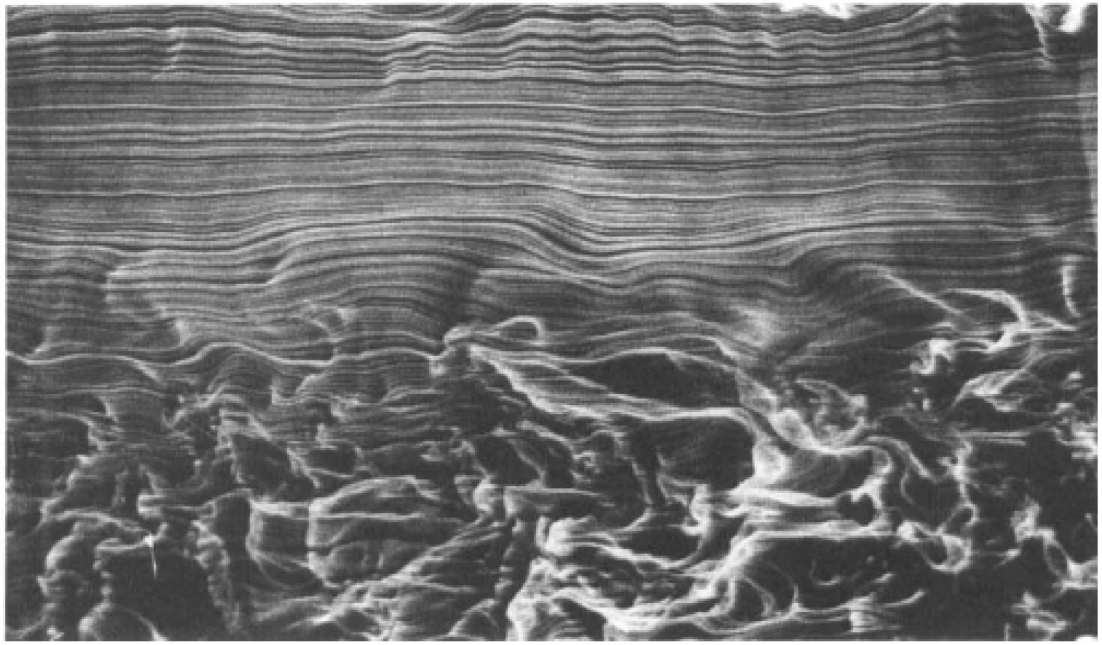

Jayesh & Warhaft,
JFM, 277, 23, 1994

Same as (a) but with
an inversion cap

(a) Homogeneous region (g+, spray side). References

Settling particle velocity enhancement and reduction in turbulence with gravity.

Alesida et al, JFM, 468 (2002)
Davila and Hunt JFM, 440 (2001)
Kawanasi and Shiozaki, J. Hydraul. Eng. 134 (2008)
Lazaro and Lasheras, Phys. Fluids, 1, (1989)
Murray, JGR, 75 (1970)
Nielsen, J. Sediment. Petrol., 35 (1993)
Tooby et al. JGR 82 (1977)
Wang and Maxey JFM, 256 (1993)
…….

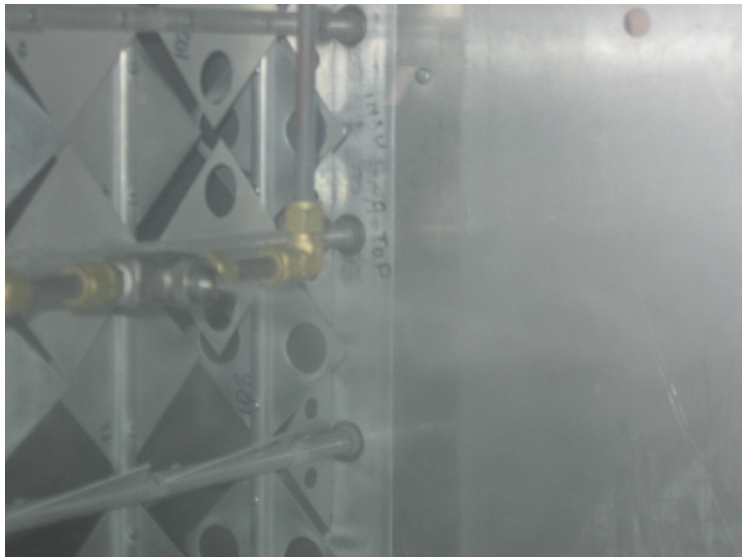

Acceleration of inertial particles:

Bodenschatz, Xu, Mordant, Ayyalasomayajula, Qureshi….

Sprays & active grid

Clustering: Shaw, Collins, Bec, Vassilicos, Hunt……

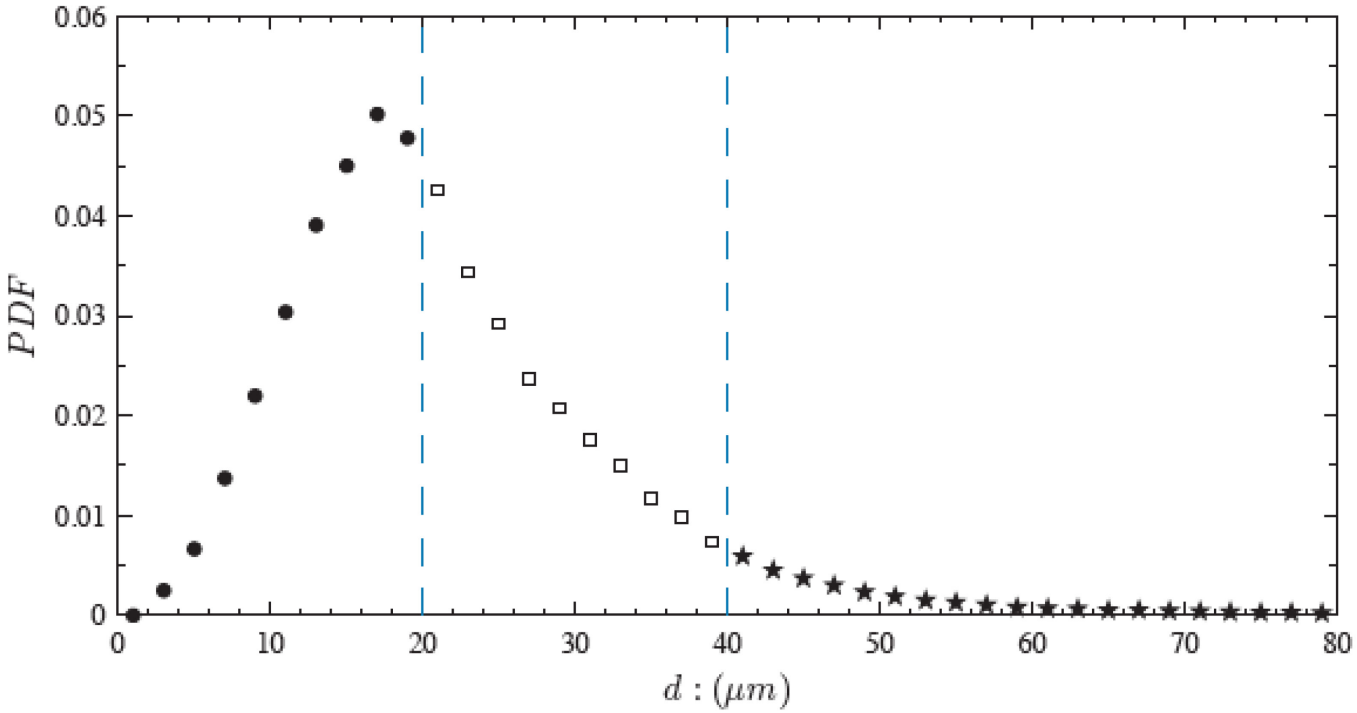

FIGURE 7. Normalized droplet probability distribution as measured in the droplet bulk ($y/l \approx 1$) at the test section. Circles, squares and stars represent the small, intermediate and large droplet groups, respectively, seperated by dashed lines. This smoother PDF was measured under nominally the same conditions as that shown in GGW, but with much increased statistics.

Droplet pdf at the measurement section

Experimental parameters

This experiment: $Re_\lambda = 275$, $St_\eta = 0.2$, $Sv_\eta = 0.54$ and $\epsilon = 0.14\,\mathrm{m^2\,s^{-3}}$,

Droplet Group	$\langle d \rangle$: (μm)	$\langle St_\eta \rangle$	$\langle Sv_\eta \rangle$	$\langle St_l \rangle$	$\langle Sv_l \rangle$
Small :	13.8(0.3)	0.061(0.002)	0.17(0.026)	$8(0.9) \cdot 10^{-4}$	0.026(0.001)
Intermediate :	27.2(0.3)	0.225(0.006)	0.61(0.01)	$3(0.3) \cdot 10^{-3}$	0.096(0.004)
Large :	51.2(0.5)	0.81(0.02)	2.2(0.3)	0.011(0.001)	0.35(0.01)
All :	22.7(0.7)	0.2(0.03)	0.54(0.01)	$2.8(0.1) \cdot 10^{-3}$	0.07(0.002)

TABLE 2. Droplet Parameters. Droplets with $d \leqslant 20$, $20 \leqslant d \leqslant 40$, and $d \geqslant 40$ μm belong to the small, intermediate, and large droplet groups, respectively.

Atmospheric measurements: Seibert, Shaw….

$Re_\lambda \; 10^3 - 10^4$, $St_\eta \sim 10^{-4} - 10^{-1}$, $Sv_\eta \sim 10^{-2} - 10^0$ and $\epsilon \sim 10^{-4} - 10^{-1}$

Kolmogorov length in experiment ~ 0.4 mm; comparable to atmosphere

Inertial Particle and Fluid Acceleration PDFs

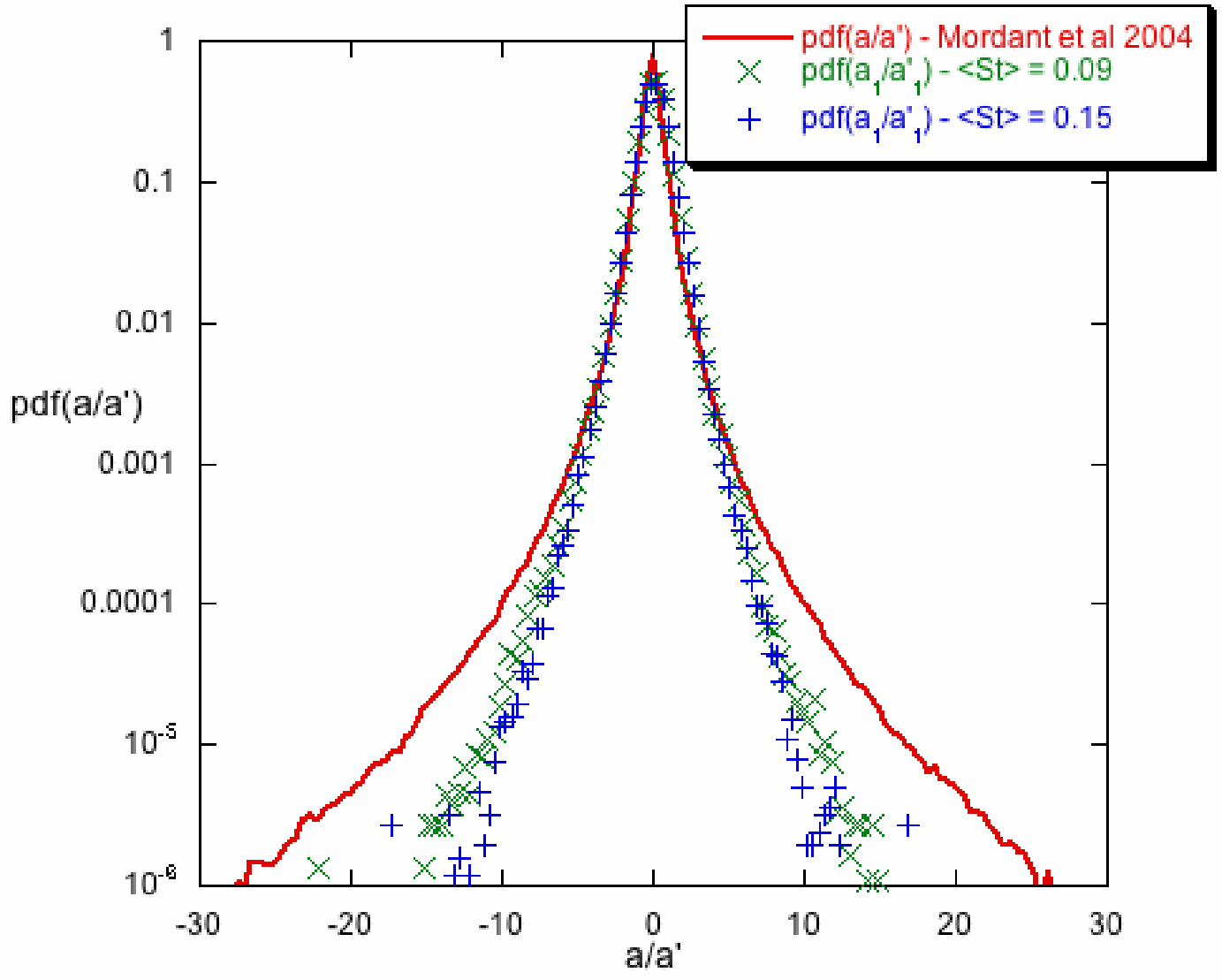

Cornell Wind Tunnel, Ayyalasomayajula et al. PRL. 2006

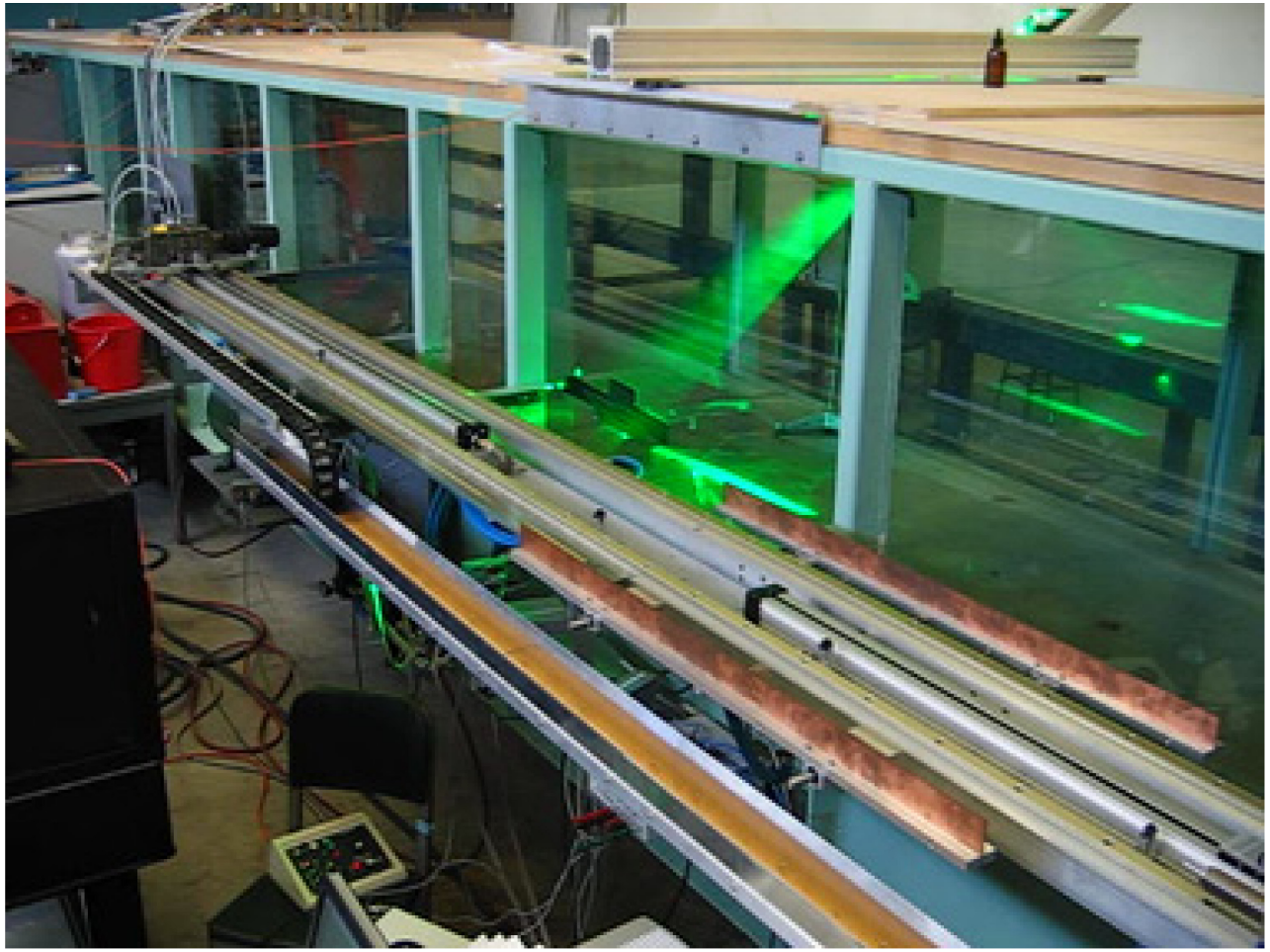

Armann Gylfason

Inertial Particles--Preferential Concentration

(Evenly distributed inertial particles concentrate in regions of high strain)

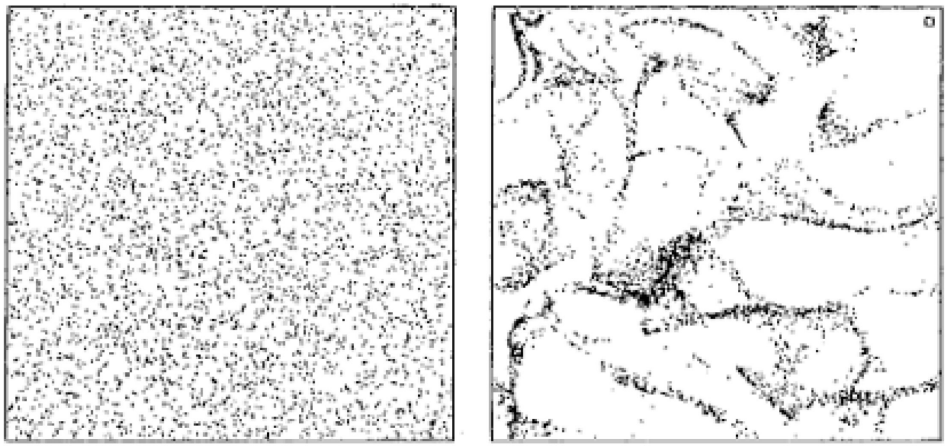

(a) (b)

From Shaw, Reade, Collins and Verliade J.A.S ,55,1998

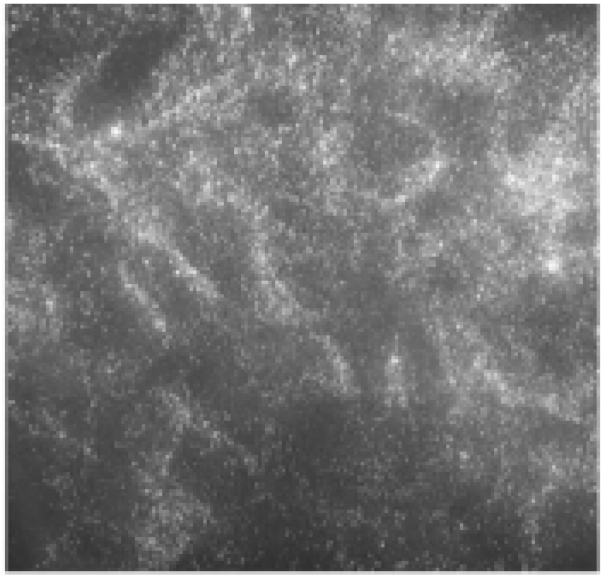

Wood et al. 2005. Glass
(20 micron) St =1.33 ,

Inertial Clustering of Particles in High-Reynolds-Number Turbulence

Ewe Wei Saw,[1] Raymond A. Shaw,[1,*] Sathyanarayana Ayyalasomayajula,[2] Patrick Y. Chuang,[3] and Ármann Gylfason[2,†]

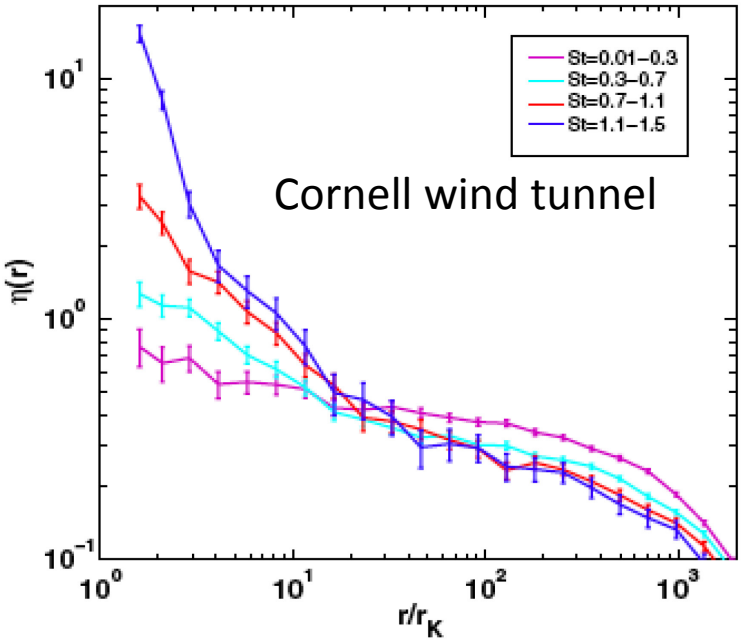

$$\eta(r) = \frac{\tilde{Q}(r)/\delta r}{Q/L} - 1, \tag{1}$$

where $\tilde{Q}(r)$ is the number of particle pairs separated by a distance within $[r - \delta r/2, r + \delta r/2]$, Q is the total number particle pairs in the sample, L is the sample length.

$$\eta(r) \propto (r/r_K)^{-f(\mathrm{St})},$$

From Kawanasi and Shiozaki,
J. Hydraul. Eng. 134 (2008)

Settling velocity in turbulence

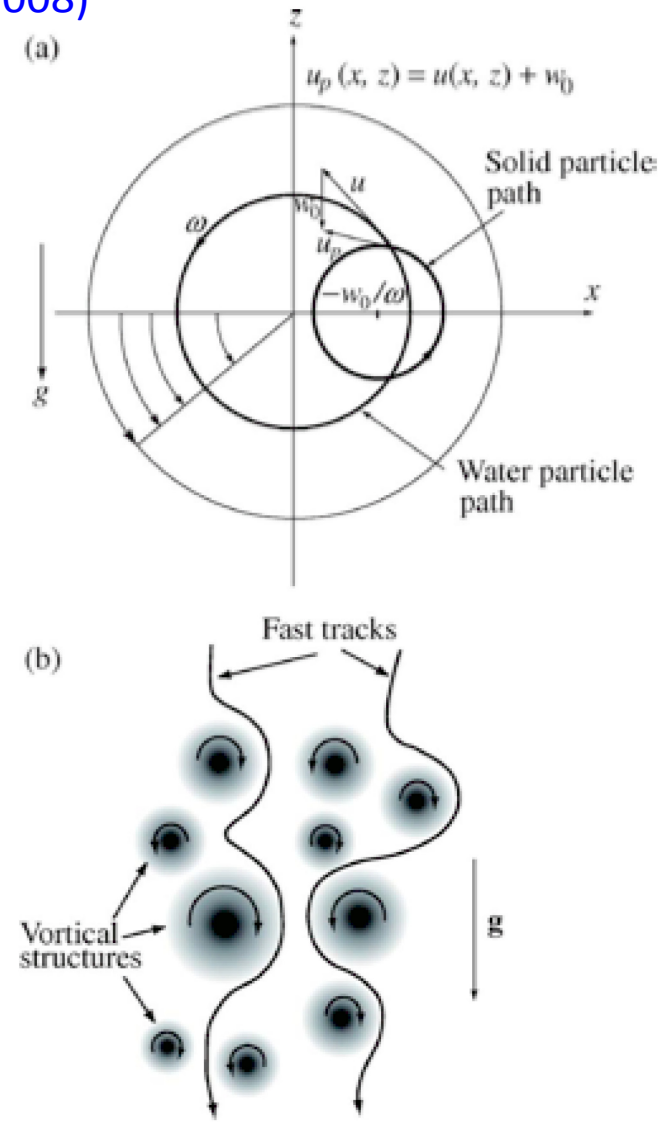

Fig. 1. Mechanisms of reduction and increase in settling velocity: (a) vortex trapping; (b) trajectory biasing and fast tracks

Tooby et al 1977

Wang and Maxey 1993

Loitering

Nelisen 1993

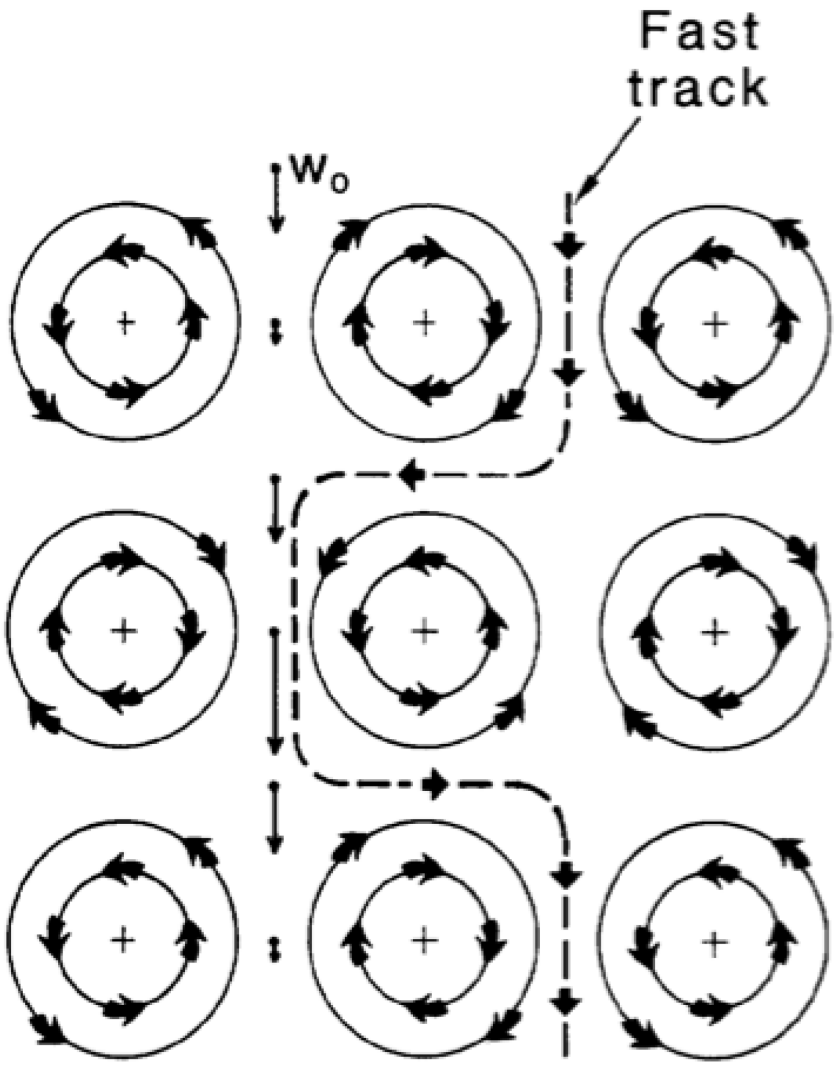

Occurs for heavy particles
in week turbulence.

Longer residence time of particles
in upward moving regions of
the flow

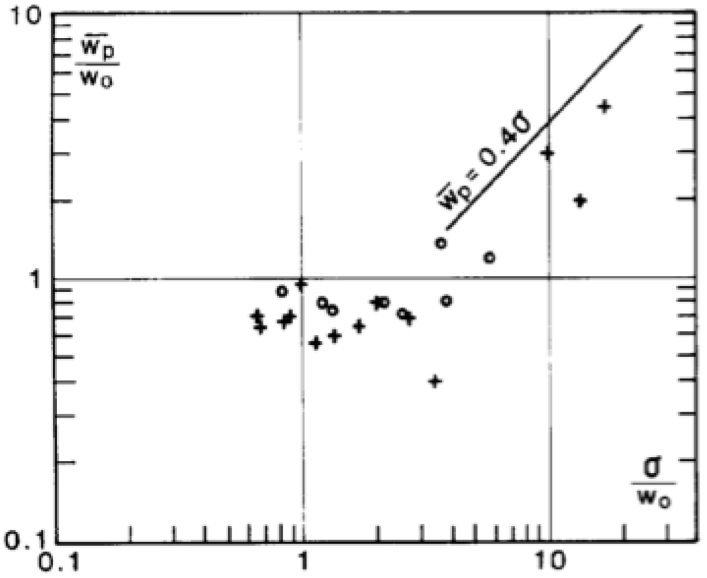

FIG. 1.—Relative settling velocity vs. relative turbulence intensity. Legend: plus signs, Murray (1970); open circles, present study.

Settling velocity vs. Settling parameter

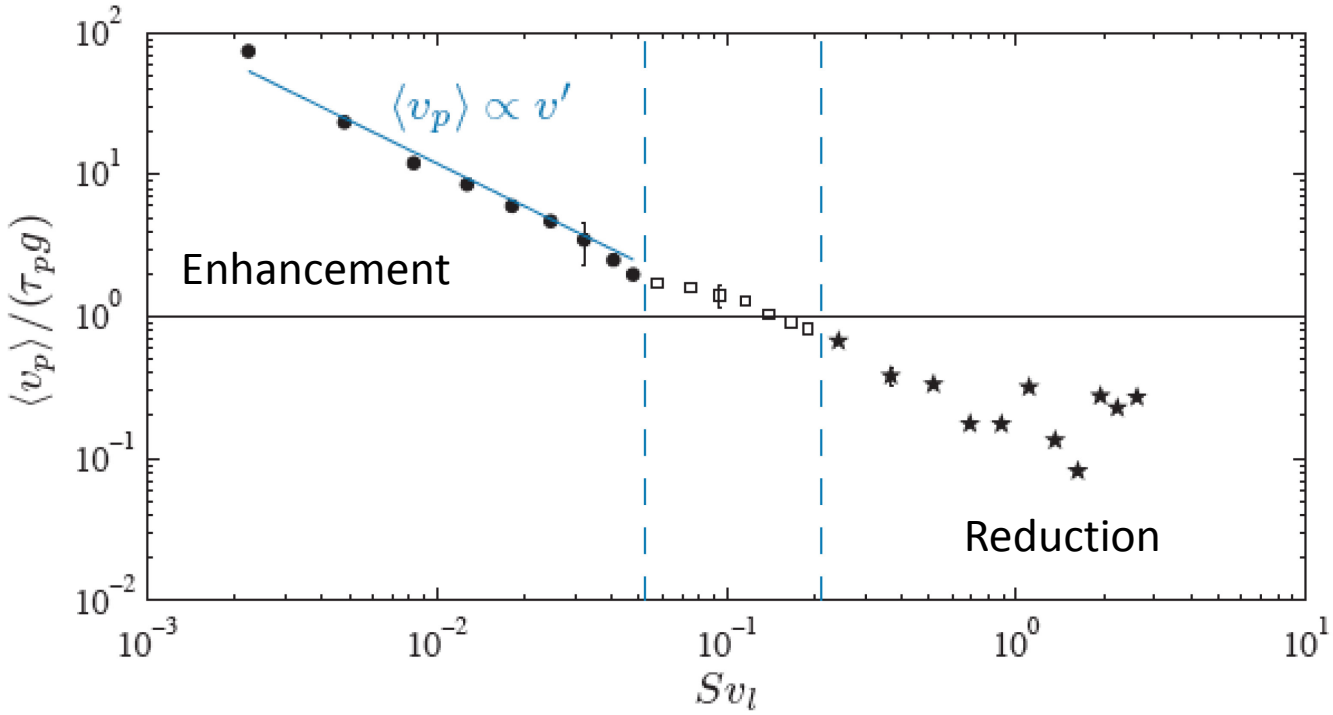

FIGURE 8. Normalized settling velocity versus settling parameter, Sv_l. Black circles, open squares and stars represent small, intermediate and large droplet groups, respectively. The abscissa progresses from relatively strong to weak turbulence, left to right.

Comparisons with other studies

$Study:$	Present	Kawanisi & Shiozaki (2008)	Aliseda *et al.* (2002)	Wang & Maxey (1993)
$Type:$	Active Grid	Flume & KS	Passive Grid	DNS
$Re_\lambda:$	275	N/A	75	$20-60$
$u'/u_\eta:$	8	N/A	$2.8-3.7$	$2.3-4.3$
$l/\eta:$	600	N/A	$180-205$	$21-33$
$d:(\mu m):$	$5-75$	$40-600$	$5-50$	N/A
$St_\eta:$	$0.007-6$	N/A	$0.01-5$	$1-2.7$
$Sv_\eta:$	$0.02-15$	N/A	$10^{-4}-0.014$	$0.4-4$
$St_l:$	$10^{-4}-.08$	$0.0003-0.06$	$10^{-3}-0.1$	$0.002-0.012$
$Sv_l:$	$10^{-3}-2.5$	$0.05-5$	<0.005	$0.1-1.7$

TABLE 3. Study Comparison. Values are approximate, and for the present study reflect the full range shown in figures 7 and 8. Those statistics which are either not available or not applicable are listed as "N/A." For Kawanisi & Shiozaki (2008), KS stands for kinematic simulation.

$$St_\eta \sim d^2 \epsilon^{1/2}$$

$$Sv_\eta \sim d^2 \epsilon^{-1/4}$$

Dávila & Hunt (2001) Settling of inertial particles near a Rankine Vortex

$Fr_p \equiv St\, Sv^2$ which is independent of ϵ

Show for $Sv < 1$ & $Fr_p \ll 1$

the turbulent settling velocity always larger than terminal vel.

For our flow: $Sv_{\text{all drops}} = 0.54$

$Fr_{p\ \text{all drops}} = 0.03$

ie expect a higher settling velocity than terminal

But for our large drops

$Sv = 2.2 \quad Fr_p = 3.4$

i.e expect the reverse

$$Fr_p \equiv St\, S_G^2$$

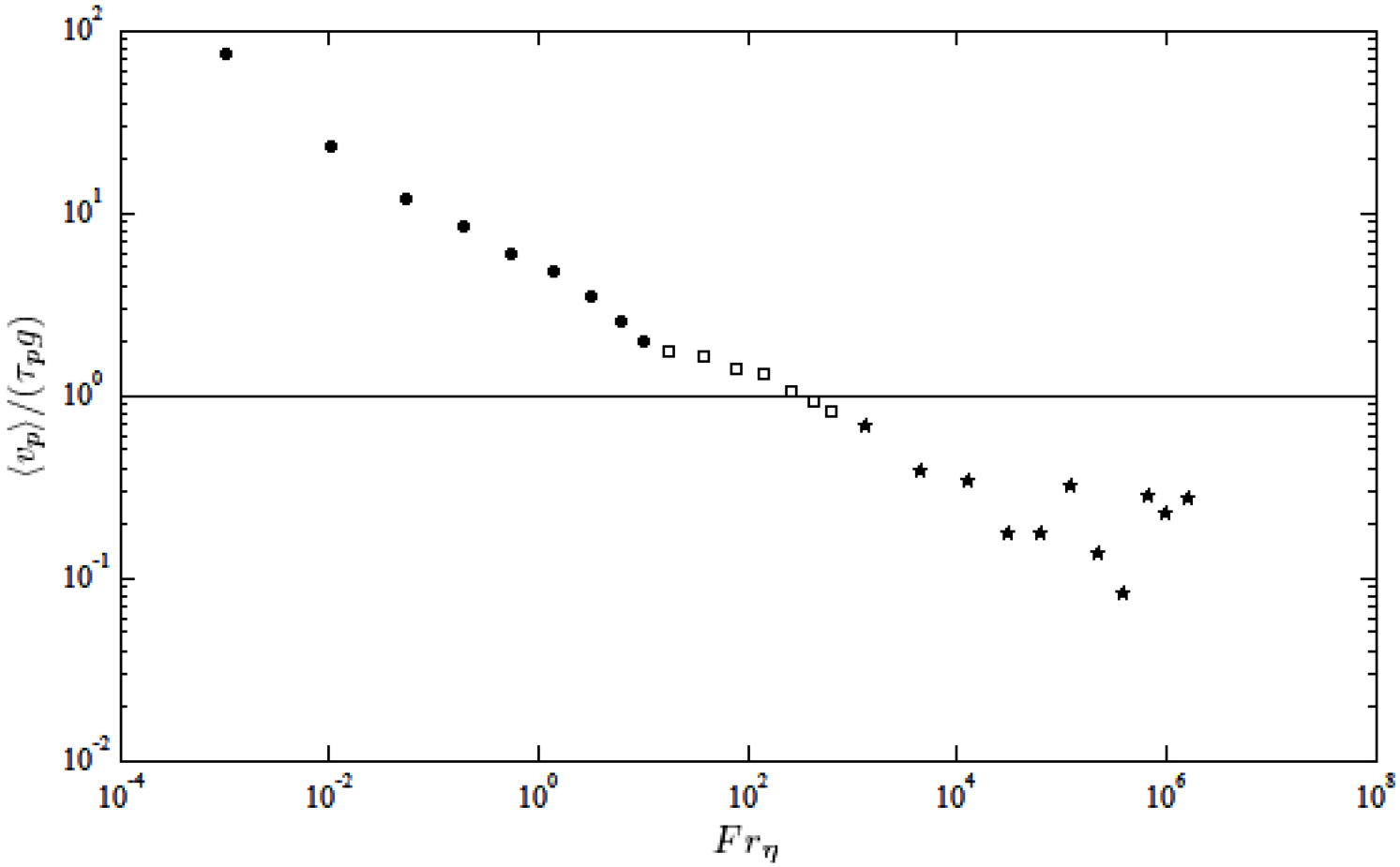

(b) Entrainment region

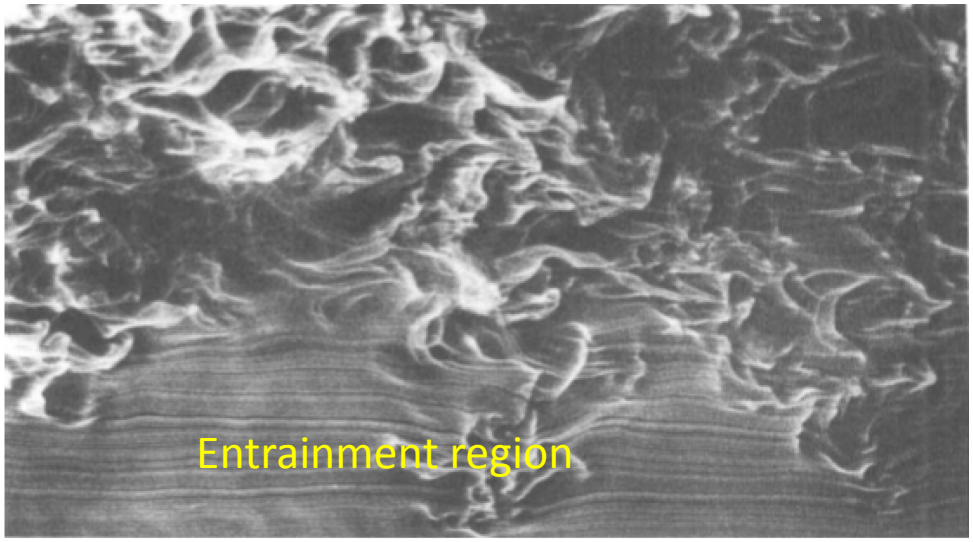

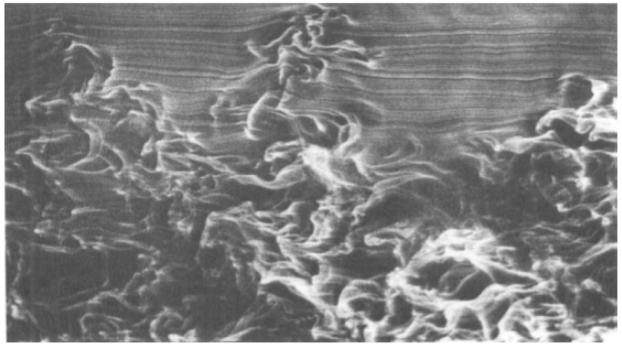

g-

g0

g+ homogeneous turbulence at the top.

Particles always injected into turbulent region

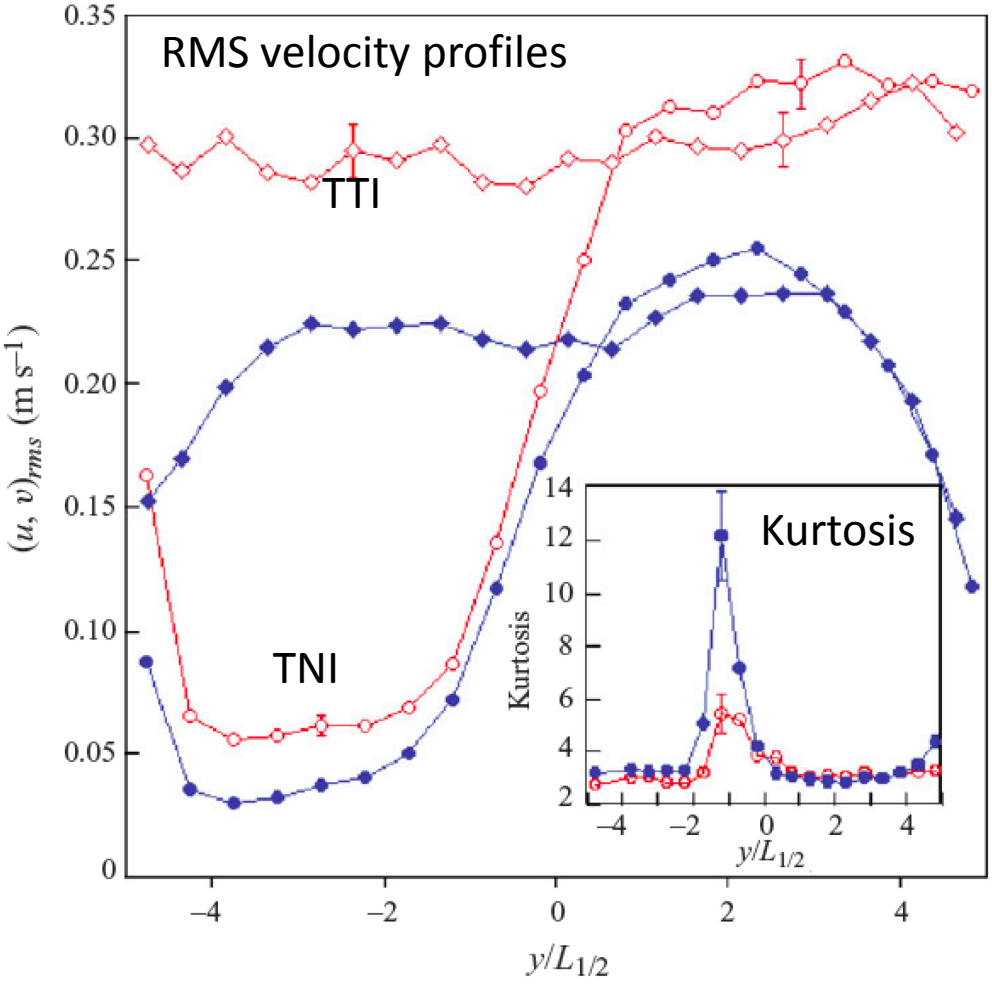

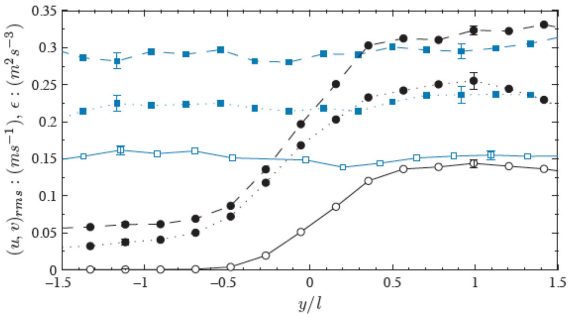

FIGURE 2. Hot-wire profiles of velocity r.m.s. and dissipation at the test section. TTI and TNI cases are squares and circles, while u and v components have dashed and dotted lines, respectively. Dissipation profiles have solid lines with open symbols.

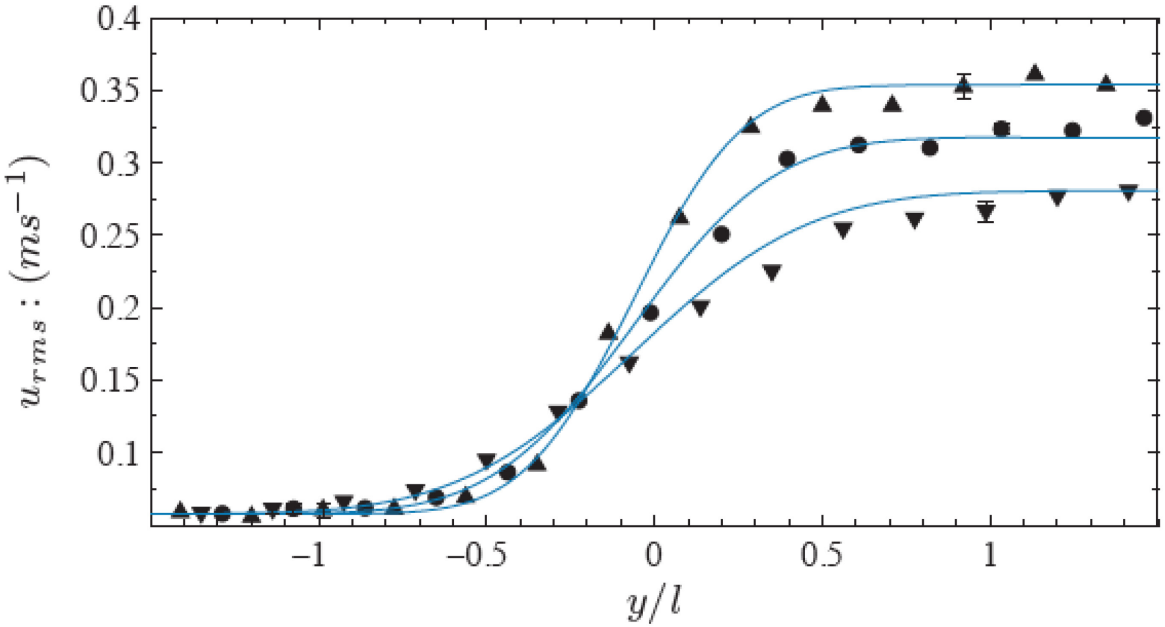

FIGURE 4. TNI profiles of u_{rms} upstream ($t/\tau_l \approx 0.4$, $x = 0.7m$), downstream ($t/\tau_l \approx 1.1$, $x = 1.8m$), and at the test section ($t/\tau_l \approx 0.7$, $x = 1.20m$), denoted by upward- and downward–pointing triangles, and circles, respectively. Lines are plots at each location of a single function in x and y adapted from the solution to 1D passive scalar diffusion with step initial conditions.

$$u_{rms}(x,y) = u'_{min} + \left(\frac{u'_{max} - u'_{min}}{2}\right)\left[1 + erf\left(\frac{y - y_o}{\sqrt{4D(x/U)}}\right)\right]$$

Velocity Spectra

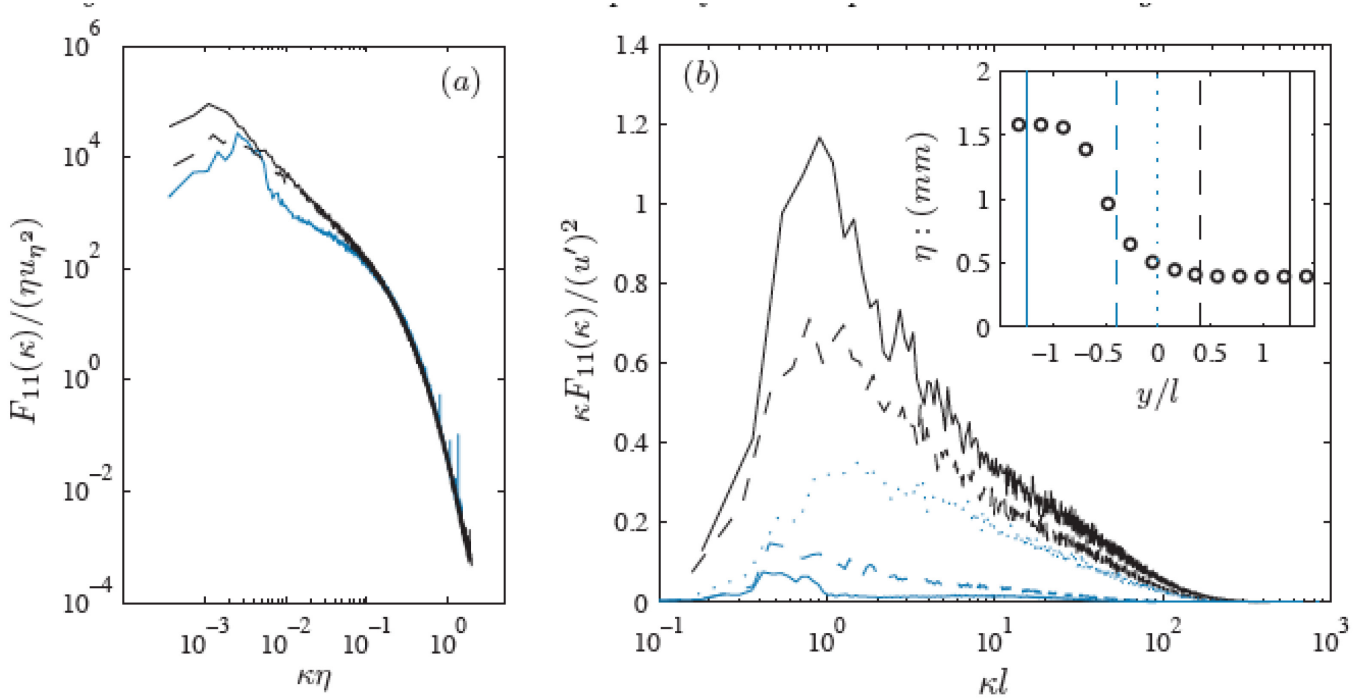

FIGURE 3. Power (a) and energy spectra (b) for the TNI, normalized with local dissipation scaling (a) and turbulence-side large eddy scaling (b). The insert shows the profile of η at the test section; vertical lines illustrate locations of the spectra in the main figures ($y/l \approx \pm 1.25, \pm 0.4, 0$), with lines from left to right in the insert corresponds to spectra from bottom to top in the figures. Only three power spectra are shown to avoid clutter from the collapse ($y/l \approx -1.25, 0.4, 1.25$).

Normalized particle concentration profiles

Without gravity, concentration profiles are insensitive to particle size.
See Gerashchenko et al. JFM, 617 (2008); Lavesso, JFM, 658 (2010)

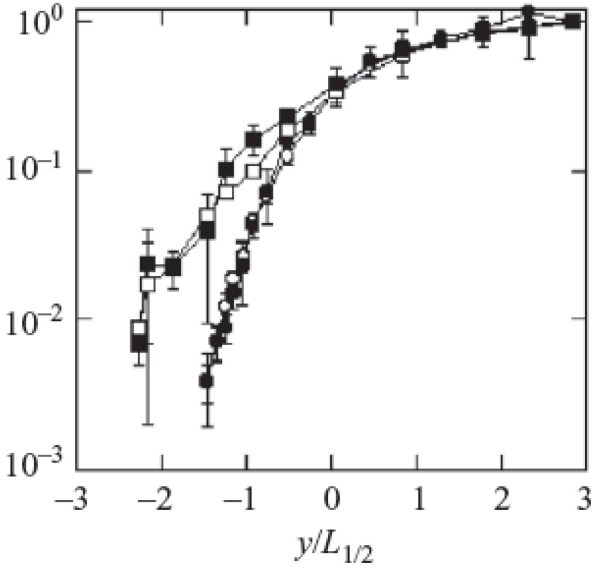

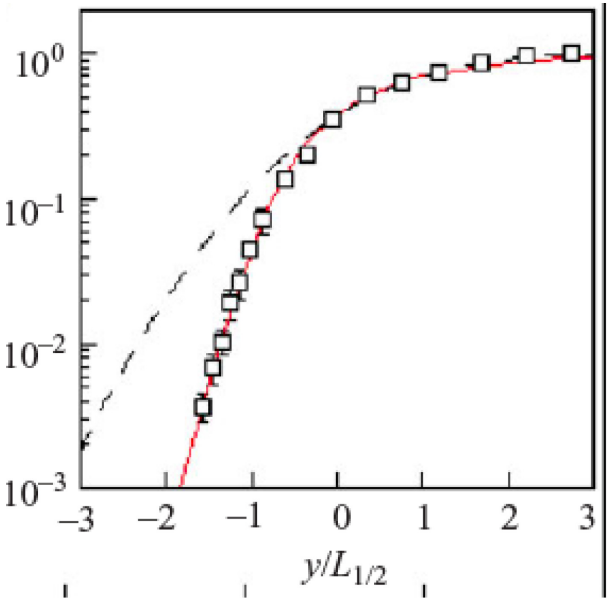

Concentration profiles for small and large particles WITHOUT GRAVITY
Upper curves: TTI, lower, TNI

An error function is observed for the TTI concentration profiles.
For the TNI, an error function is not observed

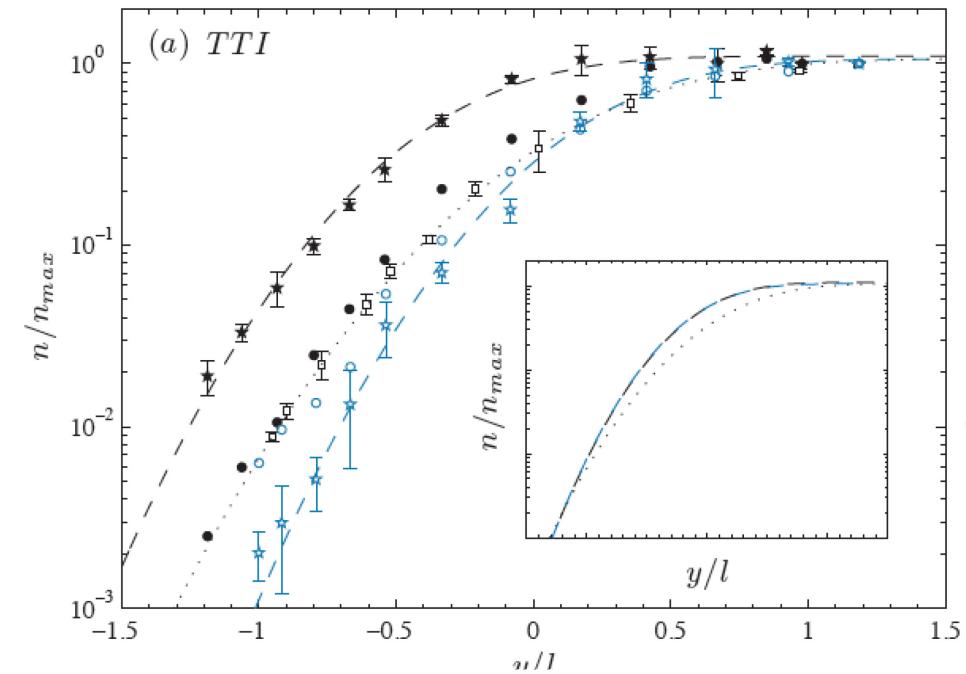

Particle concentration at the test section:

TTI: Turbulent-Turbulent Interface

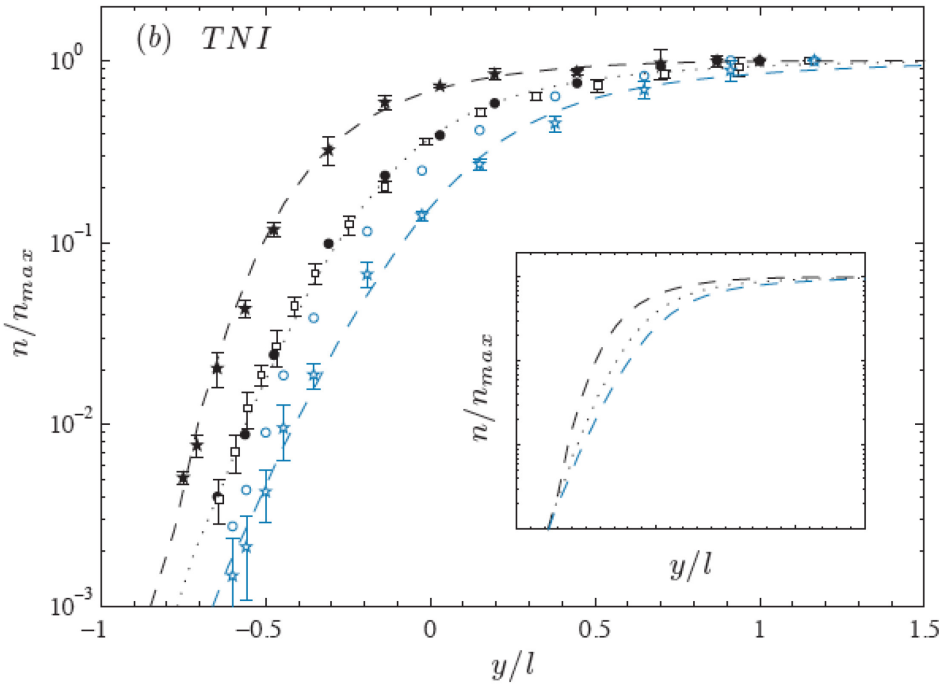

TNI: Turbulent-Non Turbulent Interface

Circles and stars: Small and large droplet groups
g+, filled symbols; g-, open symbols

Insert: curves shifted to converge asymptotically

Particle rms diameter for the TTI, TNI g+, g0, g- cases

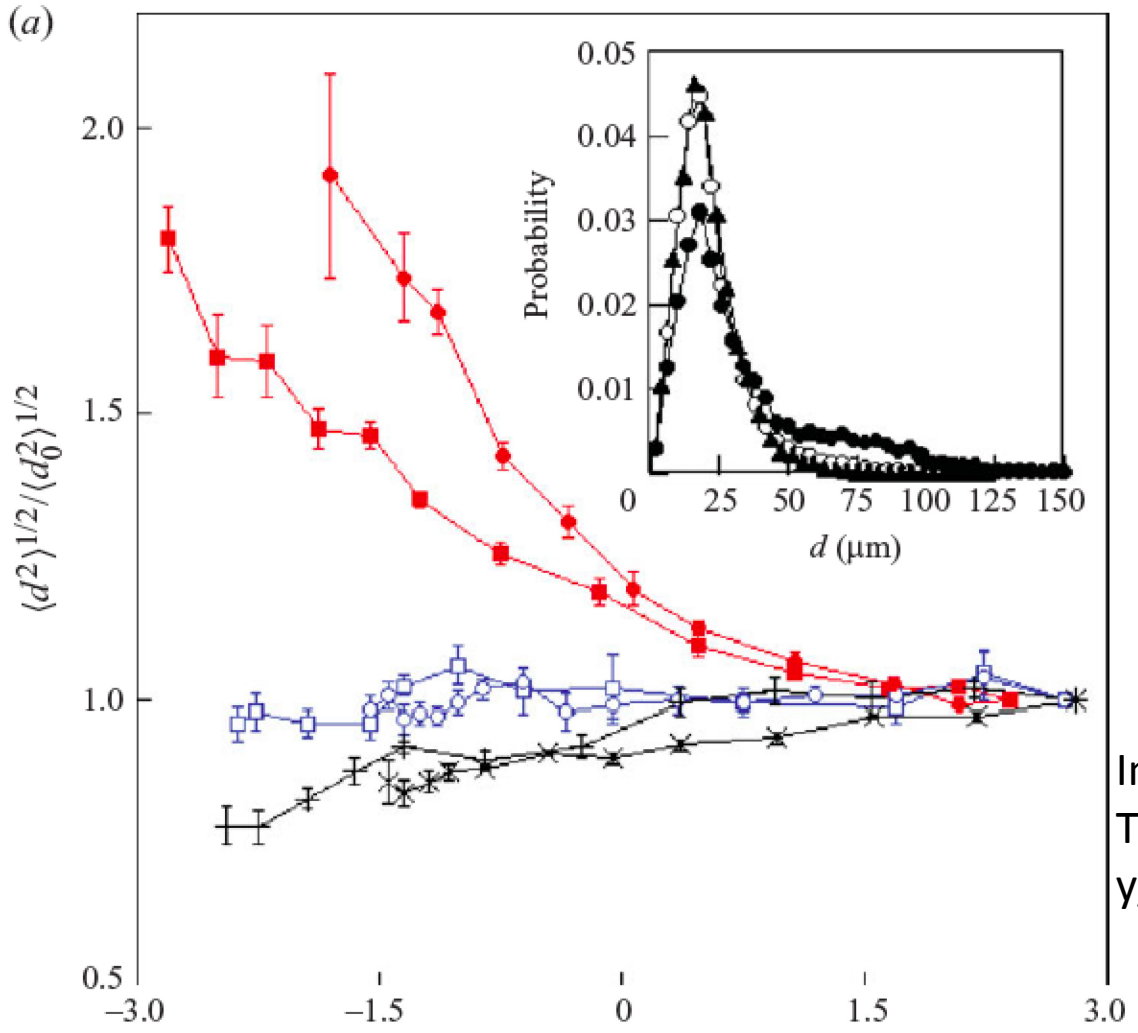

Red: g+

Blue: g0

Black: g-

Squares , TTI; circles, TNI

Insert: Particle size distributions, TNI, g+ case. y/L = 2.4 (open circles), y/L = -1.14 (filled circles)

$y/L_{1/2}$

Mean Velocity Profiles

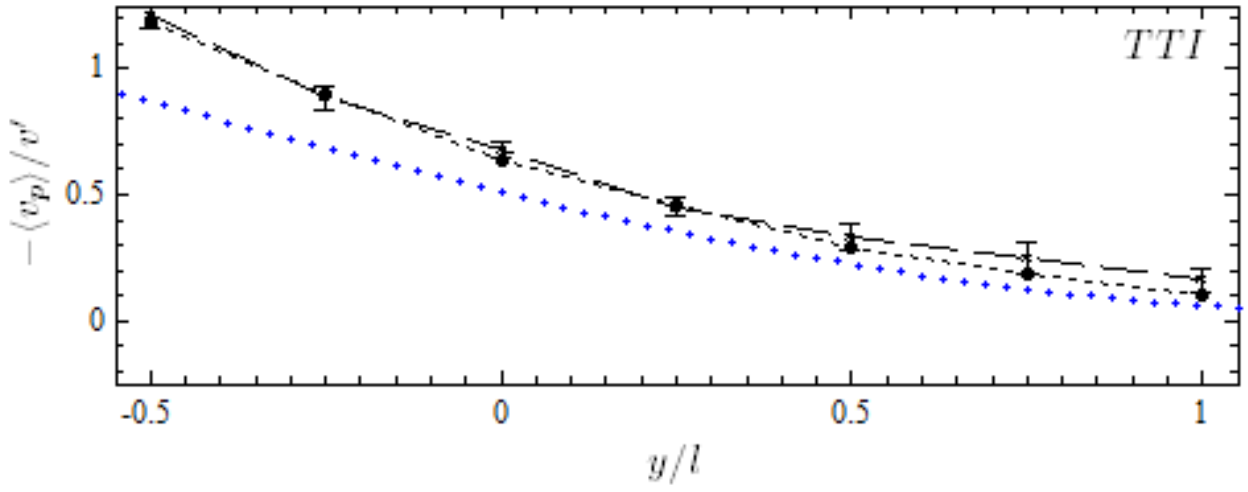

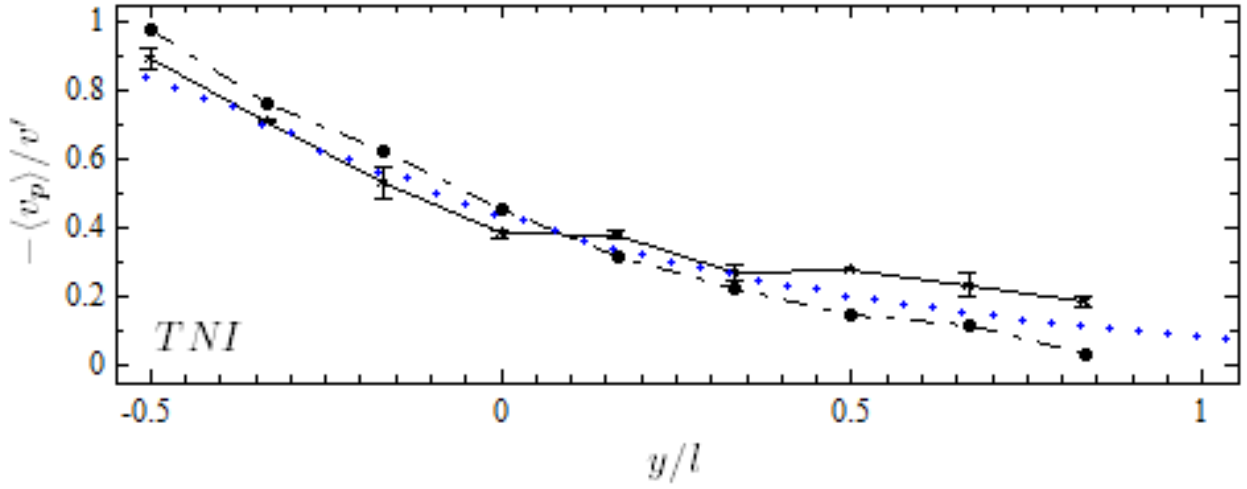

Top, TTI,

Bottom TNI.

Circles, small droplets;
Stars, large droplets

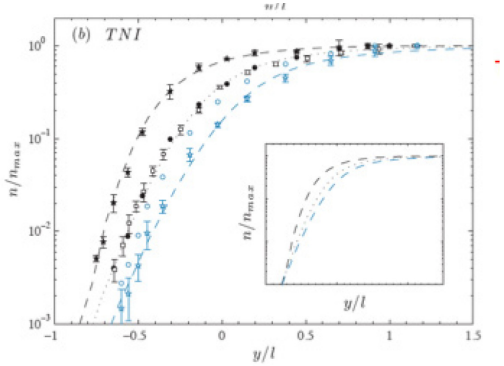

Large particle velocity diminished in entrainment region: Abscissa shift plus possible loitering.

Intermittency factor: ratio of burst time to total time

Velocity field

Turbulent
Non Turbulent
Interface. TNI

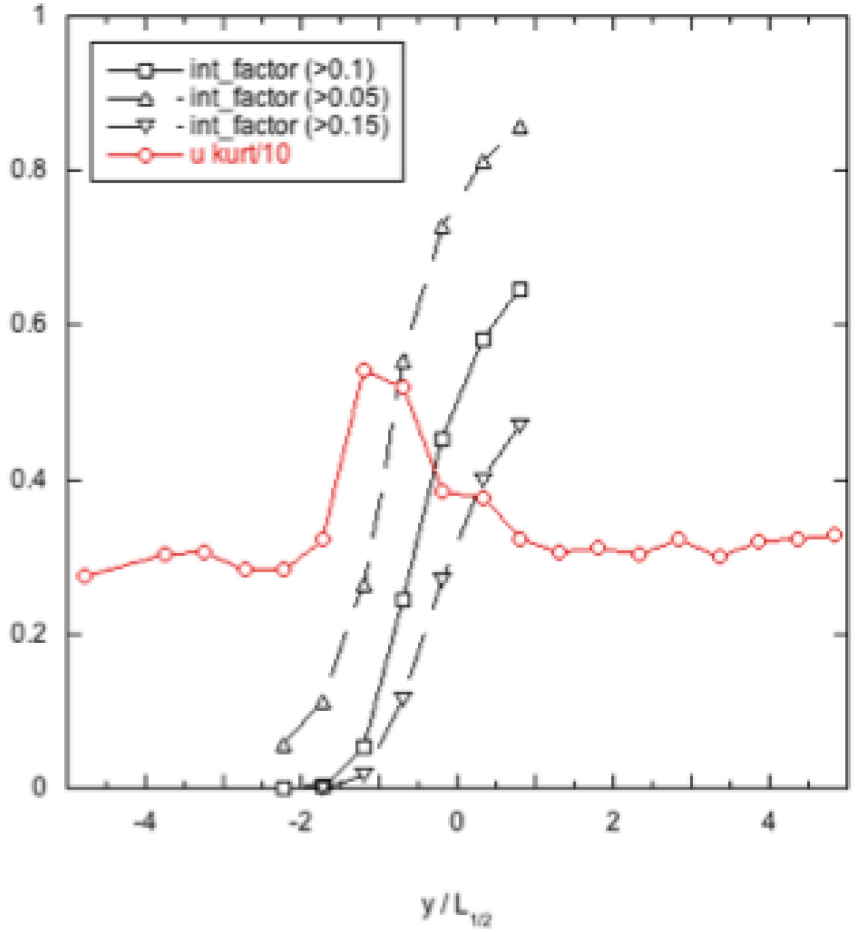

Particle velocity time series.
(a) seeded region, (b) bursting region

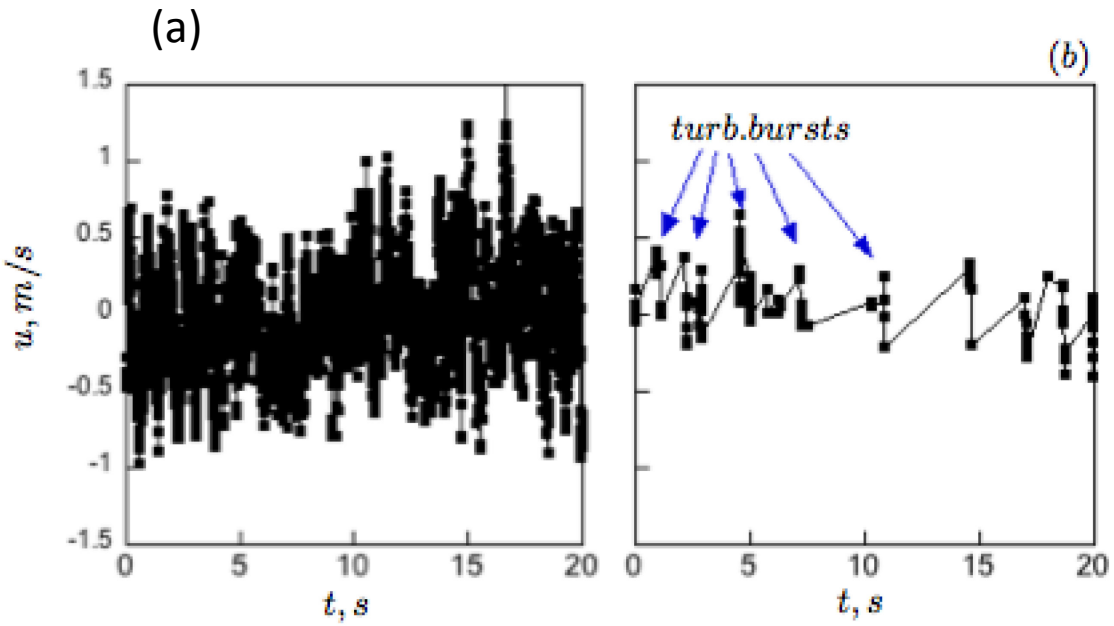

TNI case

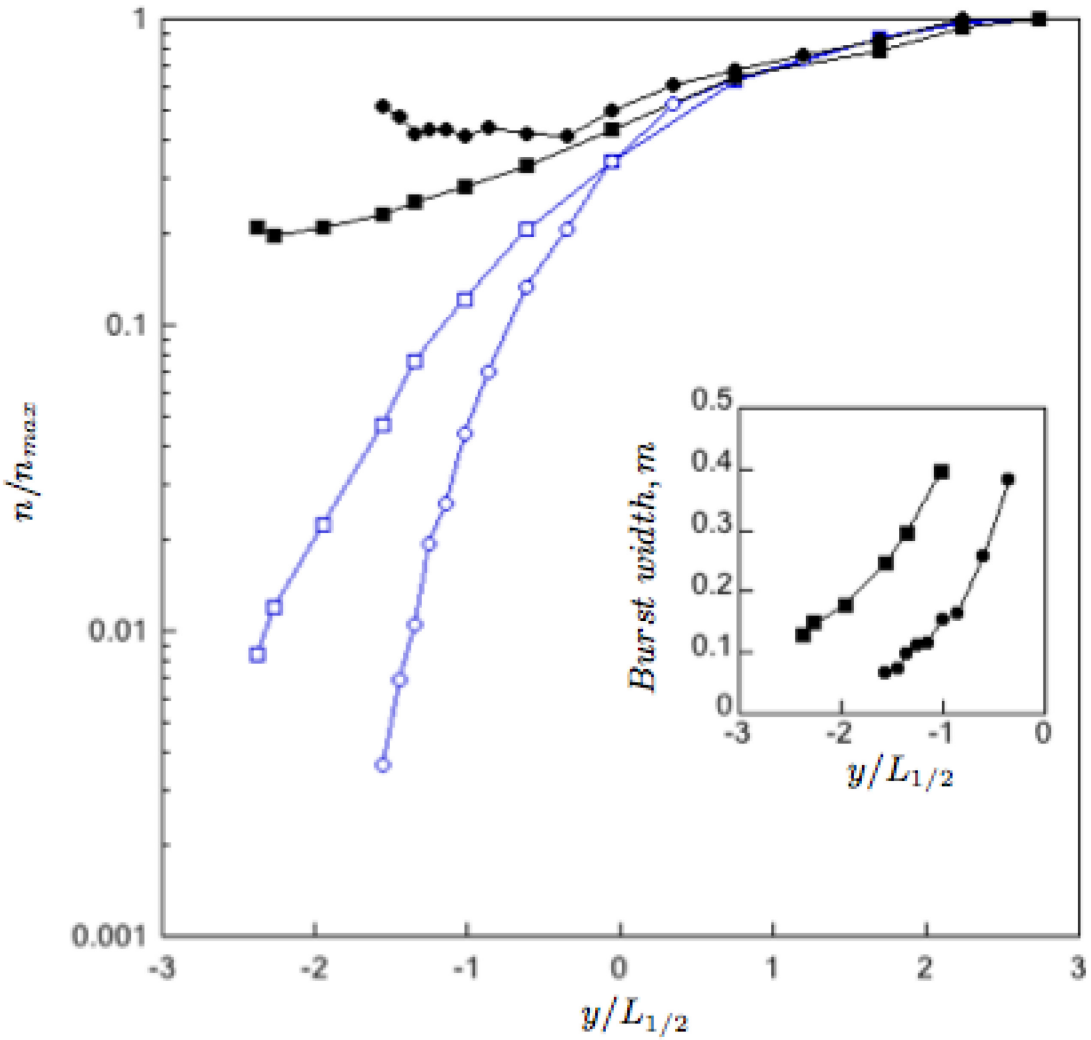

FIGURE 13. Comparison of the conditioned concentration profiles (filled symbols) and unconditioned (open symbols). Circles - TNI; squares TTI. Insert: burst width profiles in the intermittent region of the mixing layer for the TNI (circles) and TTI (squares).

Conditioned & unconditioned concentrations, no gravity

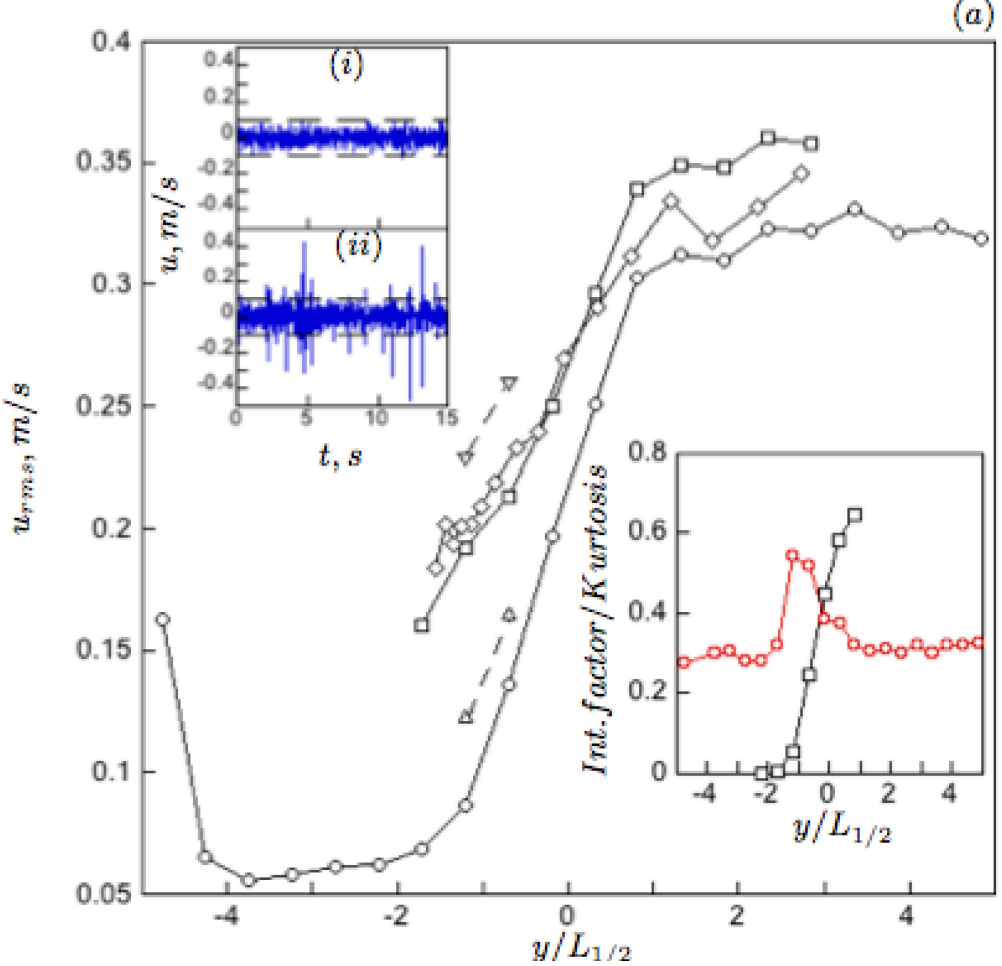

TNI. Comparison of hot wire (fluid velocity) and PDPA (Particle velocity) measurements.

Particles mainly associated with bursts.

FIGURE 10. (a) u_{rms} profiles for the TNI. Circles - unconditioned hot wire data; diamonds - PDPA data; squares - conditioned hot wire data (threshold value is $0.1m/s$). The results of applying other two thresholds are shown: triangles up - $0.05m/s$; triangles down - $0.15m/s$. Left insert: velocity time series (u components without mean, filtered with $2Hz$ high pass filter) for the TNI: (i) outside of the intermittency region where there are no bursts detected ($y/L_{1/2} = -1.2$); (ii) in the intermittency region close to the maximum of kurtosis ($y/L_{1/2} = -2.22$). Dashed lines correspond to thresholding level. Right insert: comparison of the intermittency factor (squares) and kurtosis of the u component divided by factor of 10 (circles). (b) Examples of the velocity time series measured by PDPA in the high $y/L_{1/2} = 2.7$ (left) and low $y/L_{1/2} = -1.1$ (right) turbulence sides of the TNI.

Mean droplet velocity as fn of local droplet separation distance

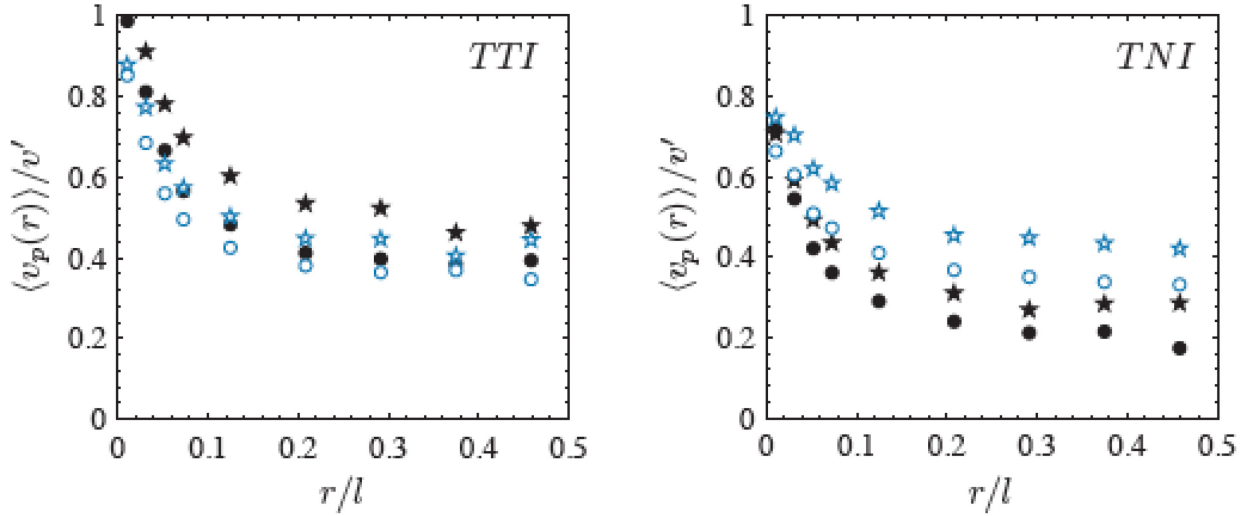

FIGURE 11. TTI (left) and TNI (right) mean droplet velocity as a function of local droplet separation distance, r, for $g+$ (filled symbols) and $g-$ (open symbols) cases. Circles and stars denote small and large droplet groups at $y/l = -1/4$.

RMS profiles of particle velocity---small particles only.

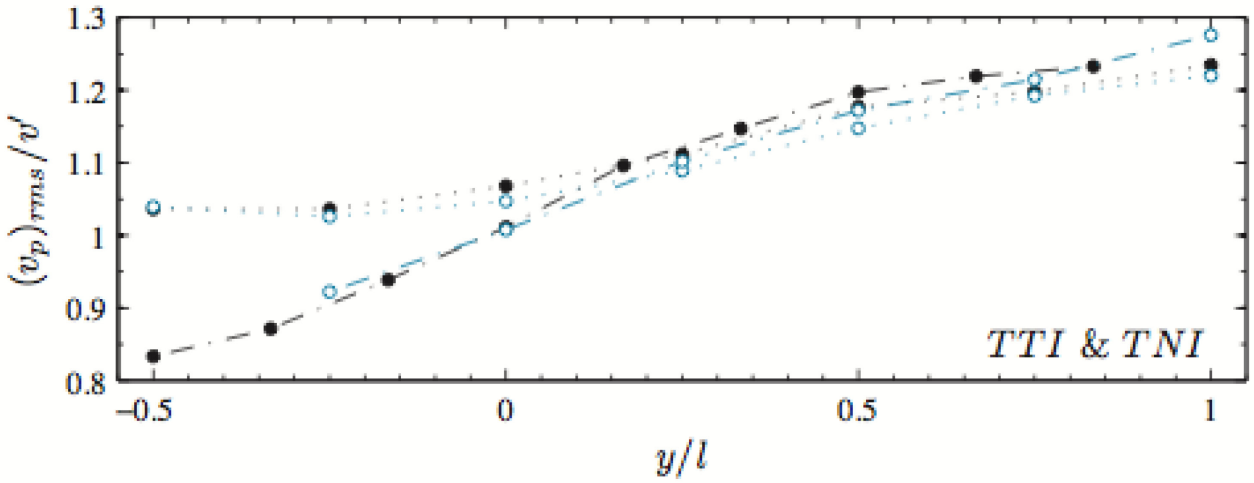

Upper curves are TTI,
Lower curves are the TNI.

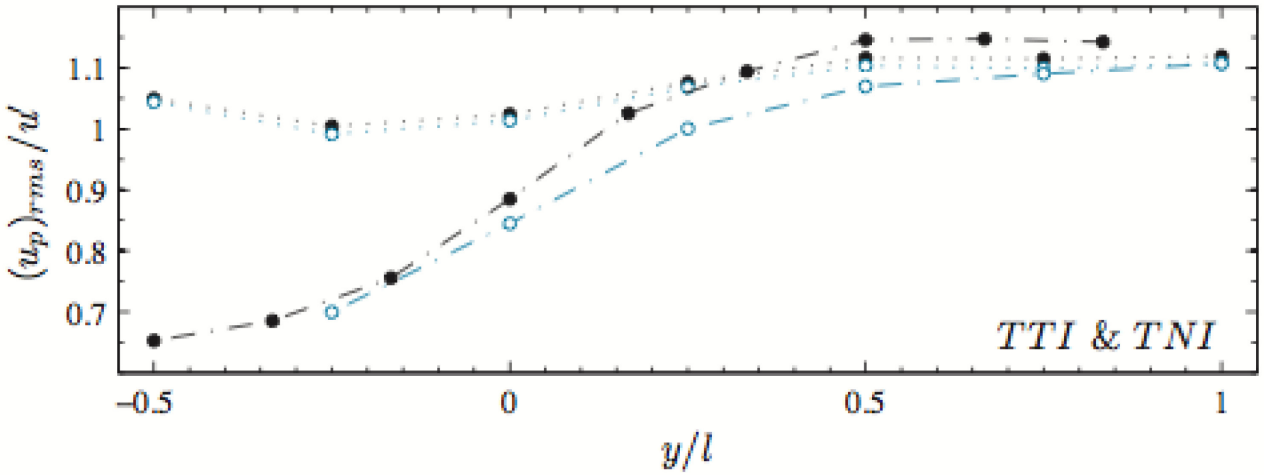

Kurtosis of the particle velocity.

Filled stars, full line: TNI, large drops, g+
Filled stars, dashed line (lower curve): TTI, large drops, g+

Open stars, blue dashed line, : TTI, large drops, g-

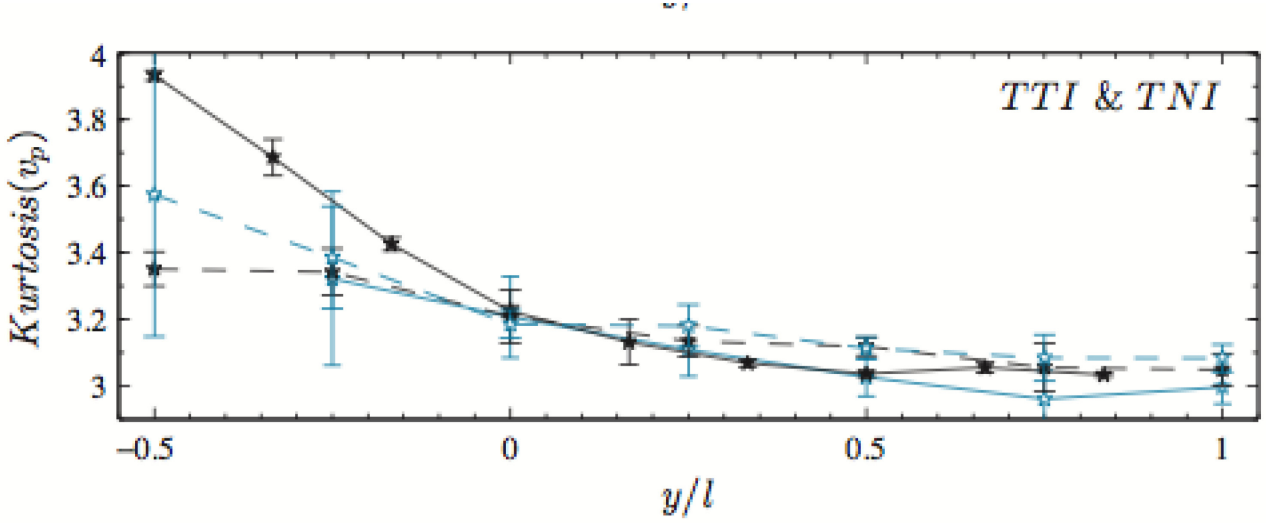

Conclusions

A reductionist approach!

Have isolated the effects of gravity and particle size.
We are attempting to add shear. ……

Results may have significance to other areas: pollution, mixing…..

Note: Ireland, P. J. & Collins, L. R. 2011 ” Direct numerical simulation of inertial particle entrainment in a shearless mixing layer.” in final preparation, confirms many of the results presented here.